Contract No:

This document was prepared in conjunction with work accomplished under Contract No. DE-AC09-08SR22470 with the U.S. Department of Energy (DOE) Office of Environmental Management (EM).

Disclaimer:

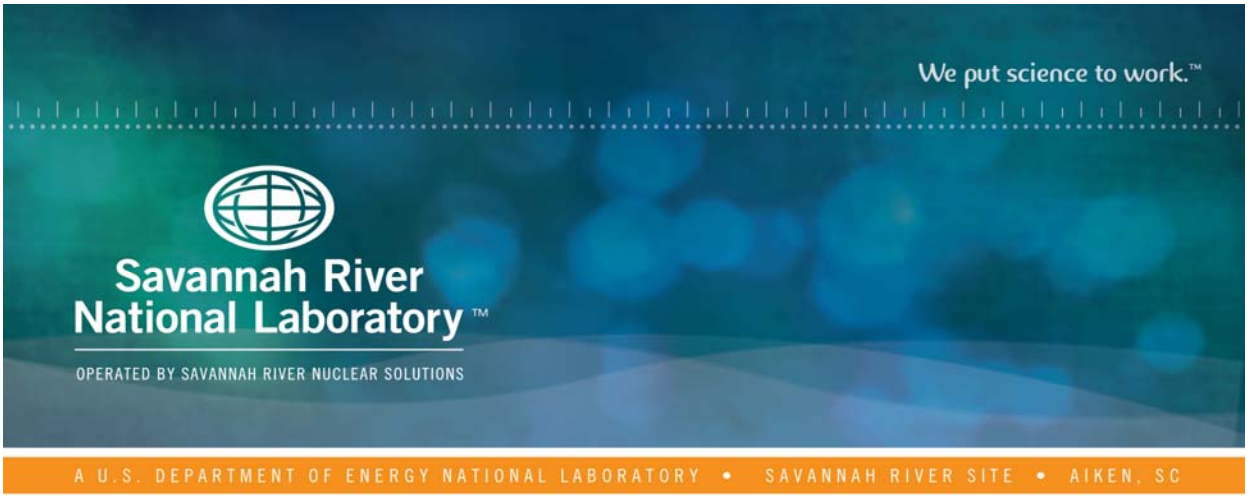

Tank Closure Cesium Removal Project CST Simulant Cesium Batch Contact Kinetics Test Results and Column Performance Predictions

William D. King, L. Larry Hamm, Charles A. Nash

May 2019

SRNL-STI-2019-00088, Revision 0

DISCLAIMER

Printed in the United States of America

Prepared for
U.S. Department of Energy

SRNL-STI-2019-00088
Revision 0

Keywords: *Salt Processing, Ion Exchange, ZAM, VERSE, TCCR*

Retention: *Permanent*

Tank Closure Cesium Removal Project CST Simulant Cesium Batch Contact Kinetics Test Results and Column Performance Predictions

William D. King
L. Larry Hamm
Charles A. Nash

May 2019

Prepared for the U.S. Department of Energy under contract number DE-AC09-08SR22470.

Savannah River National Laboratory™
OPERATED BY SAVANNAH RIVER NUCLEAR SOLUTIONS

REVIEWS AND APPROVALS

AUTHORS:

W. D. King, Advanced Characterization & Processing, SRNL Date

L. L. Hamm, Threat Assessments - National Security Date

C. A. Nash, Advanced Characterization & Processing, SRNL Date

TECHNICAL REVIEWS:

T. B. Peters, Advanced Characterization & Processing, Reviewed per E7 2.60 Date

D. J. McCabe, Wasteform Processing Technology, Reviewed per E7 2.60 Date

S. E. Aleman, TA/NSS/NS, Reviewed per E7 2.60 Date

APPROVALS:

B. J. Wiedenman, Manager, Date
SRNL, Advanced Characterization & Processing

S. D. Fink, Director Date
SRNL, Chemical Process Technology

M. T. Keefer, Date
SRR, Nuclear Safety and Engineering Integration

EXECUTIVE SUMMARY

To evaluate the cesium removal capabilities of the caustic-washed R9120-B version of crystalline silicotitanate (CST) ion exchange media from Savannah River Site (SRS) waste during Tank Closure Cesium Removal (TCCR) column processing, batch contact kinetics tests were performed at 23 °C in SRS Average simulant. Cesium loading kinetics data was also collected (in current and previous testing; King, et al., 2018a) using the same simulant for an older CST sample (IE-911) which was caustic-washed by the vendor many years ago and was recently retrieved from drums stored at SRS. (Note that R9120-B and IE-911 are believed to be identical materials, after the R9120-B was caustic washed by SRNL, and differ only by particle size and manufacturing date, and thus can be considered different batches). Although cesium loading kinetics testing can be conducted more rigorously using dynamic column tests, the batch contact method requires less simulant and considerably less experimental effort. Average percent removal data for batch contact samples for the two CST batches are provided in Table ES-1. Faster cesium uptake was observed with IE-911, although the loading rates for the two media batches were similar. After 5.5 hours of CST contact, 81% cesium removal was observed with R9120-B versus 86% removal with IE-911. Although these differences are small, the trend is consistent across the timed results, with the larger bead material always loading slower. These seemingly small differences in percent removal are believed to have a large impact on the column performance. Cesium loading curves for the two CST batches are provided in Figure ES-1 below. Faster cesium loading with IE-911 CST is presumed to be associated with the smaller average particle diameter (408 μm mean volume diameter) versus R9120-B (572 μm diameter). Cesium loading kinetic data was needed to conduct column performance comparisons (i.e., model predictions) for the two CST batches.

Table ES-1. CST Average Batch Contact Kinetics Data for TCCR Caustic-Washed R9120-B and Archived IE-911 Media with SRS Average Simulant at 23 °C.

Contact Time (hours)	1.0	1.5	5.5	24.0	96.0
	Average % Cs^+ Removal (%RSD)[a]				
R9120-B	52.0 (1.6%)[b]	---	80.6 (2.7%)	89.5 (1.1%)	93.8 (0.2%)
IE-911	---	66.8 (1.7%)[c,d]	85.5 (0.9%)[d]	92.3 (0.2%)[d]	95.1 (0.1%)[d]

[a] average and %RSD of replicate data
[b] pre-wetted CST
[c] analysis indicated that this data point may be low due to incomplete CST particle wetting during initial simulant contact
[d] data reported previously (King, et. al., 2018a)

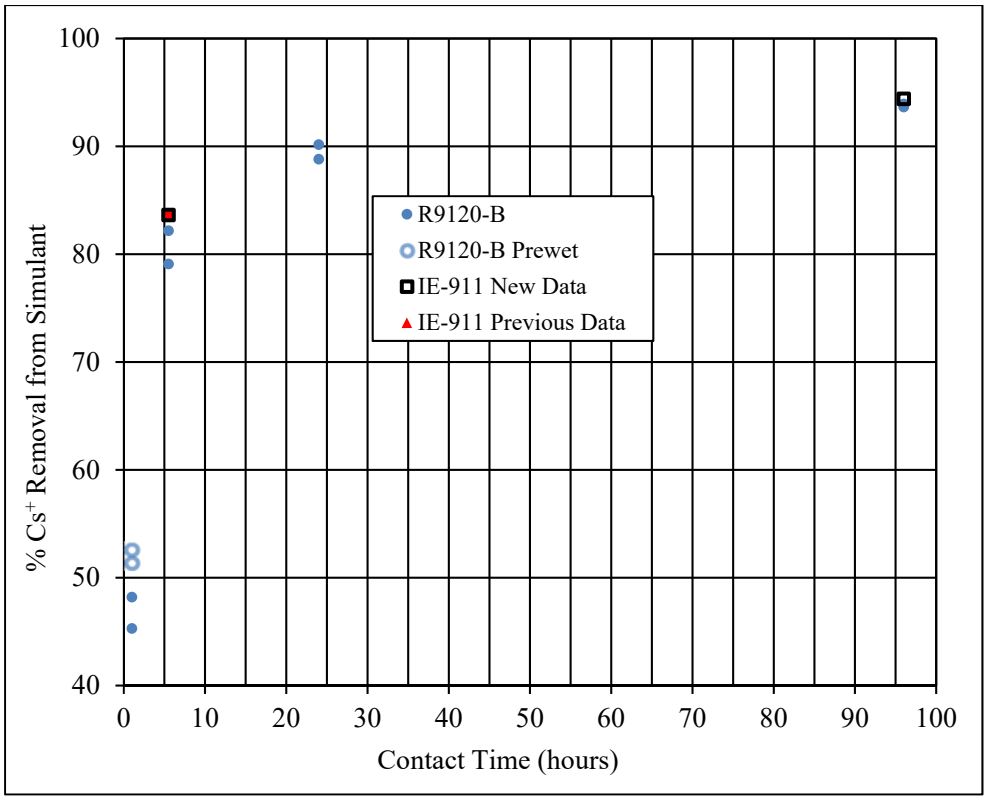

Figure ES-1. Cesium Percent Removal Versus Time for TCCR Caustic-Washed R9120-B and Archived IE-911 (current and previous data; King, et al., 2018a) Media with SRS Average Simulant at 23 ºC.

The cesium loading data was analyzed using the ZAM Isotherm and VERSE Column models. Based on the results, tau (τ) model input parameters (Hamm, et al., 2002) representing the impact of the CST particle pore path tortuosity (tortuosity factor) were determined for both media batches. A τ of 4 was selected for each batch based on the kinetics data, which indicates that the diffusivity of cesium within the CST particles is 25% of the free stream diffusivity of this ion in this simulant matrix. A τ of 4 is consistent with analysis conducted of recent PNNL column data (Hamm, et al., 2018). The fact that both media batches have approximately the same τ is also consistent with the fact that the CST batches have the same crystalline microstructure and pore geometry. Therefore, the intrinsic cesium mass transfer kinetics within the particles is believed to be the same for these CST batches. However, the average particle diameter difference between the batches is expected to lead to performance differences during column operations simply because the cesium ions must travel farther to reach all of the ion exchange binding sites in the pores of the larger beads.

Note: During document technical review, a small error (2.4%) in the measured water content of the CST was discovered which resulted in slightly lower amounts of CST in the batch contact tests on a dry mass basis than were assumed for the modeling evaluations. The corrected CST masses are provided in the report. However, since the reduced mass has a linear effect on the results and adjustments to the modeling results were expected to be minor, the decision was made not to recalculate the CST performance predictions.

Based on the analysis of the cesium loading kinetics data, it was determined that both incomplete particle wetting effects and insufficient agitation biased some short duration contact data toward lower cesium removal than expected. Subsequent short-term batch contact tests with prewetted CST media confirmed and eliminated the media wetting bias. However, it is believed that the batch contact testing method utilized for these evaluations is insufficient for short duration (≤5 hour) contacts and other methods (developed previously at SRNL; Duffey, et al., 2002) may be required to obtain accurate data for short contact times. The longer-term contact data (5.5 to 96 hours) was sufficient to derive the τ data input value.

Cesium breakthrough profiles for column operations were subsequently calculated for both CST media batches to compare cesium removal performance under dynamic flow conditions. Calculated cesium breakthrough profiles are provided in Figure ES-2 for planned experimental conditions where it is apparent that significantly faster breakthrough is expected for the R9120-B CST. The calculations are based on a single column case, while TCCR operations are expected to involve at least two columns in series. For the single column operation, approximately 2.5 times more waste simulant volume can be processed with IE-911 CST than with the R9120-B media at a flow rate of 3 column bed volumes per hour (BV/hr) when targeting a cesium decontamination factor (DF) of 1000 (instantaneous breakthrough basis). For TCCR multiple column operations, the impact of the CST batch will be lower than predicted for the single column case.

Waste volume processing rate effects on cesium breakthrough profiles with R9120-B CST were also calculated using the VERSE model as shown in Figure ES-3, where it is apparent that decreasing the flow rate from 6 to 1 BV/hr results in a large increase (~6.5x) in volume processed before reaching the target DF. Slower waste processing flow rates can obviously be used to compensate for the impact of larger particle diameter in R9120-B CST. Other analysis indicated that temperature effects on column performance had minimal influence on waste volume processed to reach the DF across the range of 23-40 °C. Column performance sensitivity studies were also conducted for the tortuosity factor parameter and correlations between the tortuosity factor and the particle size metric selected were determined.

Future studies should consider the use of a cesium standard of known concentration to evaluate the possibility that analytical uncertainty is contributing to the variability in CST binder dilution factor for a given CST batch. We recommend sieve data and the Sauter mean metric as the standard protocol for the CST average particle diameter. It would be useful to establish a standard test protocol to check the kinetics performance of CST batches including a CST pre-wetting step. Consistent preparation and use of simulants are recommended. Side-by-side column tests with the two media batches under identical conditions are recommended and planned since this is the best and preferred method of performance comparison.

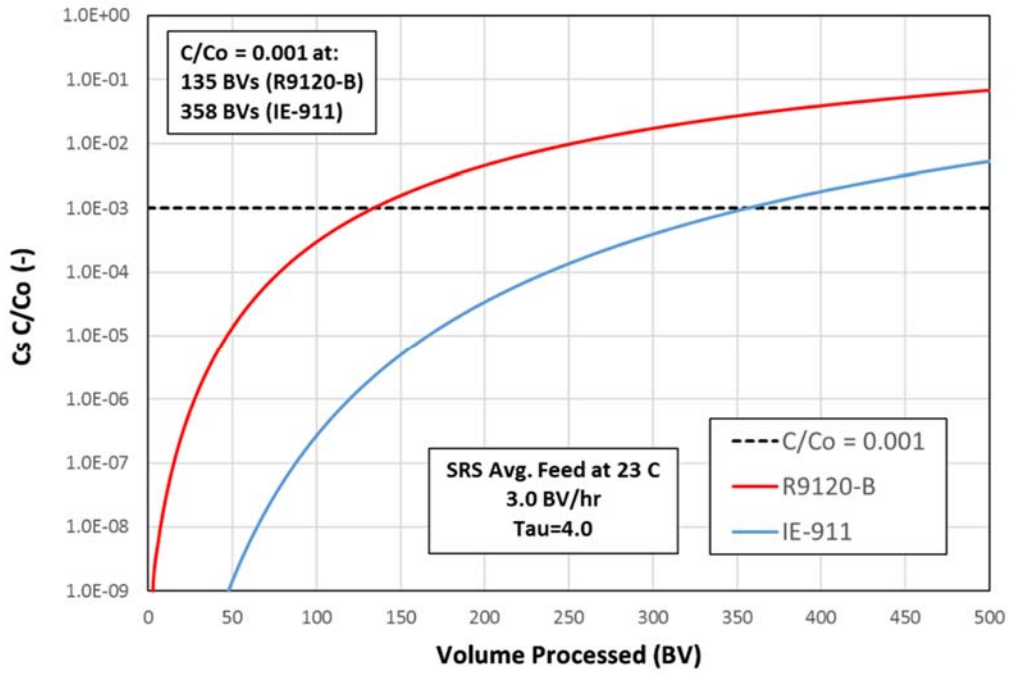

Figure ES-2. VERSE predicted basecase Cs^+ breakthrough curves based on single columns using IE-911 and R9120-B CST materials with SRS Average Simulant feed at 23°C (semi-log plot).

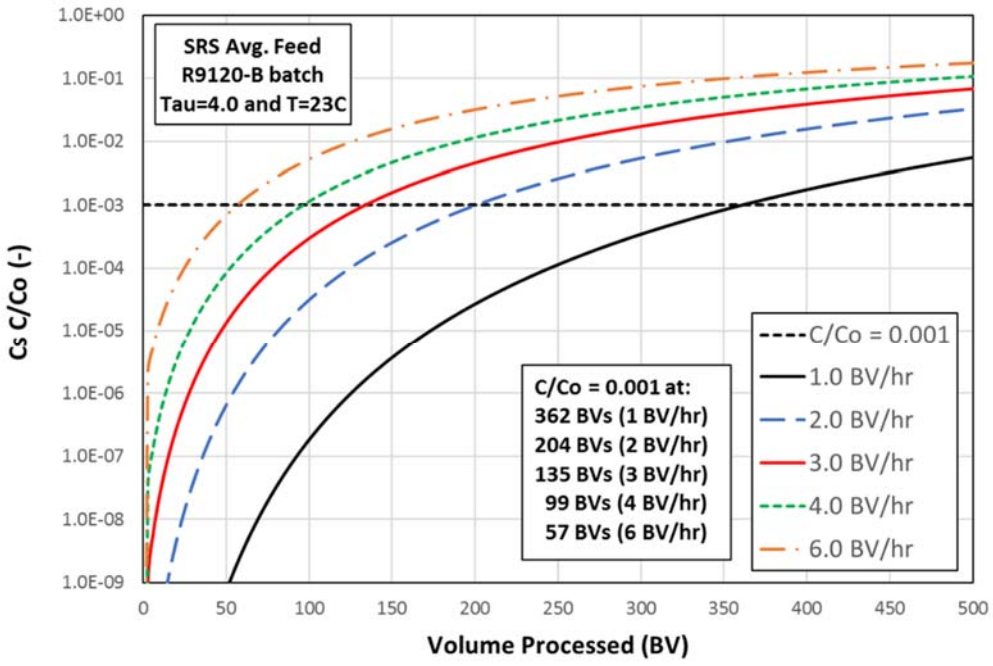

Figure ES-3. VERSE predicted flowrate impact on Cs^+ breakthrough curves based on single columns using R9120-B CST material with SRS Average Simulant feed at 23°C (semi-log plot).

TABLE OF CONTENTS

LIST OF TABLES x
LIST OF FIGURES x
LIST OF ABBREVIATIONS xiii
1.0 Introduction 1
1.1 Quality Assurance 1
2.0 Experimental Methods and Modeling Approach 2
2.1 CST Media Pretreatment and Sample Collection Methods 2
2.2 CST Physical Property Measurements for R9120-B 3
2.3 Computation of Particle Diameter Statistics Based on Sieve Analysis Data 3
2.4 Simulant Preparation 4
2.5 Batch Contact Test Equipment 4
2.6 CST Batch Contact Testing with SRS Average Simulant 4
2.7 ZAM Isotherm Model Calculations 5
3.0 Results and Discussion 6
3.1 Physical Property Measurements for R9120-B and IE-911 CST 6
3.2 CST Loading Batch Contact Kinetics Tests with SRS Average Simulant 11
3.3 Test Result Comparisons with Modeling 15
4.0 Conclusions 19
5.0 Recommendations 20
6.0 References 21
Appendix A . CST Isotherm Analyses using ZAM 23
Appendix B . CST Particle Kinetics 29
Appendix C . CST Column Predictions/Performance 37

LIST OF TABLES

Table ES-1. CST Average Batch Contact Kinetics Data for R9120-B and IE-911 Media with SRS Average Simulant. v

Table 2-1. SRS Average Simulant Composition Developed by Walker. 4

Table 2-2. SRS Average Simulant Composition Charged Balanced for use in ZAM Predictions. 6

Table 3-1. Vendor R9120-B Sieve Size Analysis Results 6

Table 3-2. Computed Log-Normal Distribution of R9120-B Particle Size Based on Vendor Sieve Analysis. 8

Table 3-3. Microtrac Particle Size Analysis Data for R9120-B CST Media. 9

Table 3-4. Cesium Loading Versus Time Test Results with R9120-B CST and SRS Average Simulant at 23 °C. 13

Table 3-5. Cesium Loading Versus Time Test Results with IE-911 CST and SRS Average Simulant at 23 °C. 14

Table 3-6. Strontium Analysis Results for Feed and Batch Contact Solutions. 15

Table 3-7. Vendor R9120-B Sieve Size Analysis Results. 10

Table 3-8. Computed Log-Normal Distribution of IE-911 Particle Size Based on Vendor Sieve Analysis 11

LIST OF FIGURES

Figure ES-1. Cesium Percent Removal Versus Time for TCCR Caustic-Washed R9120-B and Archived IE-911 Media with SRS Average Simulant at 23 ºC. vi

Figure ES-2 VERSE predicted basecase Cs^+ breakthrough curves based on single columns using IE-911 and R9120-B CST materials with SRS Average Simulant feed at 23°C (semi-log plot). viii

Figure ES-3 VERSE predicted flowrate impact on Cs^+ breakthrough curves based on single columns using R9120-B CST material with SRS Average Simulant feed at 23°C (semi-log plot). viii

Figure 3-1. Computed Particle Diameter Fit to CST R9120-B Vendor Sieve Data. 7

Figure 3-2. Microtrac Particle Size Analysis Results Plot for R9120-B CST Media. 8

Figure 3-3. Optical Microscope Image of R9120-B CST Media. 9

Figure 3-6. Computed Particle Diameter Fit to CST IE-911 Vendor Sieve Data 11

Figure 3-5. Cesium Percent Removal Versus Time for Caustic-Washed R9120-B and IE-911 Media with SRS Average Simulant at 23 ºC. 14

Figure 3-6. Cesium Loading on Solid Phase Versus Time from SRS Average Simulant on CST at 23 °C. 14

Figure 3-7. Approach, along an operating line, to equilibrium for the R9120-B engineered-form CST media in contact with SRS Average Simulant at 23 °C. 16

Figure 3-8. CST particle kinetic data versus VERSE modeling highlighting impact on particle size and batch differences. 17

Figure 3-9. VERSE predicted basecase Cs breakthrough curves based on single columns using IE-911 and R9120-B CST materials with SRS Average Simulant feed at 23°C (semi-log plot). 18

Figure 3-10. VERSE predicted flowrate impact on Cs breakthrough curves based on single columns using R9120-B CST material with SRS Average Simulant feed at 23°C (semi-log plot). 19

Figure A-1. ZAM based binary Cs^+ isotherm for SRS Average Simulant at 23°C and CST in its powdered-form (IE-910). 23

Figure A-2. Temperature dependent beta-factor for binary Cs^+ isotherm for SRS Average Simulant and CST in its powdered-form (IE-910). 24

Figure A-3. Comparison of equilibrium batch contact data versus ZAM predictions for various engineered-form CST media in contact with SRS Avg simulant at 23 °C. 25

Figure A-4. Approach, along an operating line, to equilibrium for the IE-911 engineered-form CST media in contact with SRS Average Simulant at 23 °C. 27

Figure A-5. Approach, along an operating line, to equilibrium for the R9120-B engineered-form CST media in contact with SRS Average Simulant at 23 °C. 28

Figure B-1. Cartoon illustrating the various mass transfer mechanisms occurring at a specific CST particle. 29

Figure B-2. Cartoon illustrating the basic elements of a batch contact test. 30

Figure B-3. CST (R9120-B) particle kinetic data versus VERSE modeling highlighting film versus pore diffusion contributions. 31

Figure B-4. CST particle kinetic data versus VERSE modeling highlighting impact on particle size and batch differences. 32

Figure B-5. CST particle kinetic data versus VERSE modeling highlighting tortuosity factor impact. 33

Figure B-6. CST particle kinetic data versus VERSE modeling highlighting tortuosity factor impact at intermediate contact times. 34

Figure B-7. CST particle kinetic data versus VERSE modeling highlighting the rapid mass transfer rates at early times. 34

Figure B-8. Relationship between tortuosity factor value and what particle size metric chosen. 35

Figure B-9. Simple correlation between tortuosity factor and particle size metric for CST IE-911 material. 36

Figure C-1. Diagram showing a two-column and a three-column configuration in VERSE. 37

Figure C-2. VERSE predicted basecase Cs breakthrough curves based on single columns using IE-911 and R9120-B CST materials with SRS Average Simulant feed at 23°C (semi-log plot). 39

Figure C-3. VERSE predicted basecase Cs breakthrough curves based on single columns using IE-911 and R9120-B CST materials with SRS Average Simulant feed at 23°C (linear plot). 39

Figure C-4. VERSE predicted temperature impact on Cs breakthrough curves based on single columns using R9120-B CST material with SRS Average Simulant feed (semi-log plot). 40

Figure C-5. VERSE predicted temperature impact on Cs breakthrough curves based on single columns using R9120-B CST material with SRS Average Simulant feed (linear plot). 40

Figure C-6. VERSE predicted tortuosity factor impact on Cs breakthrough curves based on single columns using R9120-B CST material with SRS Average Simulant feed at 23°C (semi-log plot). 41

Figure C-7. VERSE predicted flowrate impact on Cs breakthrough curves based on single columns using R9120-B CST material with SRS Average Simulant feed at 23°C (semi-log plot). 42

Figure C-8. VERSE predicted flowrate impact on Cs breakthrough curves based on single columns using R9120-B CST material with SRS Average Simulant feed at 23°C (linear plot). 42

LIST OF ABBREVIATIONS

BDF	CST Binder Dilution Factor
BV	Column Bed Volume
CDF	Computed Diameter Fit
C_i	Initial concentration
C_f	Final concentration
CST	Crystalline Silicotitanate
DF	Decontamination Factor
F	F-factor for water correction of CST mass
HLW	High Level Waste
ICP-ES	Inductively Coupled Plasma – Emission Spectroscopy
ICP-MS	Inductively Coupled Plasma – Mass Spectroscopy
K_d	Distribution Coefficient (ml/g dry CST)
M	Molarity (moles solute/liter solution)
m	mass
MS	Mass Spectroscopy
OLI	OLI Systems Thermodynamic Model
ϕ	Liquid:solid phase ratio (mL/g)
Q	Ionic loading (mmol/g dry CST)
RPM	Revolutions per Minute
SQAP	Software Quality Assurance Plans
SRNL	Savannah River National Laboratory
SRR	Savannah River Remediation
SRS	Savannah River Site
τ	Tortuosity factor
TCCR	Tank Closure Cesium Removal
TGA	Thermal Gravimetric Analysis
TTQAP	Task Technical and Quality Assurance Plan
UOP	Honeywell Universal Oil Products
V	Volume (mL)
VERSE	VERSE column model
wt %	Weight percent
ZAM	ZAM Isotherm Model

1.0 Introduction

At-tank ion exchange processing of Savannah River Site Tank 10H waste commenced in January 2019. The Tank Closure Cesium Removal project is focused on dissolving the waste (primarily sodium saltcake solids) within the tank followed by at-tank treatment of the waste using columns of crystalline silicotitanate ion exchange media. Four TCCR columns have been prepared, loaded with CST, and installed at SRS. The CST media loaded into the columns has a larger average particle diameter than historical media batches evaluated at SRS. Models have been developed to predict both equilibrium cesium loading on CST in High Level Waste (HLW) supernate solutions and column performance (cesium breakthrough) during waste processing. Evaluations of the impact of larger particle size and CST batch on the performance of the TCCR columns are needed to select the best operational strategy for processing the Tank 10H waste. The larger CST bead particle size is expected to impact cesium loading kinetics. As a result, batch contact kinetics tests have been performed using an average SRS waste simulant. The results have been analyzed to refine model input parameters for this CST batch and compare column breakthrough performance predictions to an earlier production batch still available at SRS. Calculated cesium breakthrough profiles are provided for experimental columns planned to validate the model predictions.

In addition to batch contact kinetics tests, the bulk density and particle size of the primary TCCR CST media batch were measured to provide needed characterization data for model input. The batch contact filtrate samples were also analyzed for strontium (Sr^{2+}). Although strontium was not added to the simulant, it is a common impurity in laboratory chemicals which strongly competes with Cs^{+} for CST ion exchange sites.

1.1 Quality Assurance

Requirements for performing reviews of technical reports and the extent of review are established in Manual E7, Procedure 2.60. SRNL documents the extent and type of review using the SRNL Technical Report Design Checklist contained in WSRC-IM-2002-00011, Rev. 2. The work was performed following the applicable TTQAP, Technical Task and Quality Assurance Plan [King, 2018b]. The Technical Task Request (TTR) associated with this work [Fellinger, 2018] indicates that portions of this work are Safety Significant, but that the testing reported herein and the supporting modeling are for production support rather than technical baseline and are not Safety Significant (see section entitled “Clarification of Safety Significant Tasks”). The software packages used as part of this work scope must comply with 1Q, QAP 20-1 Software Quality Assurance, E7, Section 5.0 and Software Engineering and Control, Applicable provisions of Section 5.4, Procedure 2.31, E7 Manual. Data are recorded in the Electronic Laboratory Notebook (ELN) system as notebook/experiment number A2341-00117-11.

The OLI Studio™ is an acquired software that meets the commercial grade definition criteria in accordance with Manual E7 Procedure 3.46 and is accepted from the vendor by verifying the parts identifiers are correct. Dedication of the commercial grade software in accordance with Manual E7, Procedure 5.07 is not required for the OLI software, which was classified as Level D [Choi 2001]. Therefore, OLI calculations meet the production support needs specified for this task in the TTR. All the activities related to the verification and validation of the OLI software database and the resulting models were documented in accordance with Manual E7 Procedure 5.40, Software Testing, Acceptance and Turnover.

SRNL was provided with two executable files (i.e., “CSTIEXV4.EXE” and “Cstiexv5.exe”) of the ZAM program running on the PC platform. Version “Cstiexv5” includes some improvement to

better account for strontium effects. It is however numerically less stable than version "CSTIEXV4". ZAM was developed to function under MS Windows XP and older versions of Windows. For newer Windows version (e.g., Windows 7, Windows 10), emulators are required to provide XP functionalities for ZAM to run. Without emulators, ZAM will not run in Windows versions newer than Windows XP. ZAM is currently classified as Level D software [Tamburello, 2011] and ZAM calculations meet the production support needs specified for this task in the TTR. The functional requirements placed on ZAM Versions 4 and 5 were verified and validated [Hamm et al., 2001].

Prior to applying VERSE-LC to the ion exchange modeling a verification process was completed and the results of that effort were reported in Hamm et al. (1999). The verification process ensures that the installed Windows version of VERSE-LC (i.e., version 7.80) was capable of adequately solving the above-mentioned governing equations and provided guidelines on how to accurately use the VERSE-LC code (e.g., mesh refinement requirements and input/output options). For all column simulations, numerical errors associated with the results of VERSE-LC should be very small when compared to the uncertainties associated with various model input parameters (bed density, particle size, pore diffusion, etc.). VERSE-LC was classified as Level D (Hang 2017) and VERSE calculations meet the production support needs specified for this task in the TTR.

2.0 Experimental Methods and Modeling Approach

2.1 CST Media Pretreatment and Sample Collection Methods

A bottle of CST media was received for testing at SRNL labeled as IONSIV[a] R9120-B, Lot #2099000034, Mat. #8103701-556, Sub-sample from CUA #125953-A. This CST lot and another lot (#2099000035) were used to fill the TCCR columns installed at SRS, with Lot #2099000034 being the dominant batch (~87 wt. %). The CST sub-sample was pretreated in the laboratory as described previously (King, et al., 2018c) to produce CST beads in the standard reference state (caustic washed, air dried at 35 °C to constant mass, and stored under ambient conditions). The pretreated CST was transferred to an approximately 4-inch diameter glass crystallizing dish and sub-samples for each batch contact test were collected with a spatula as a composite of beads removed from multiple locations (≥4) around the vessel.

A sample of IE-911 CST Lot #2081000056 (Mat. #80562-556p, Drum #36232-1-5) stored for many years at SRS was collected from a drum (described in detail in an earlier report, King, et al., 2018a) and sub-sampled for batch contact testing as described above for R9120-B CST. The IE-911 media had been provided by UOP in the caustic-washed, sodium form and was not further preconditioned or treated by SRNL prior to testing. Although IE-911 media is often preconditioned in the laboratory, this batch had already been preconditioned by the vendor so this as-received condition (but after ~17 years storage) is defined as the reference state for this media batch. The IE-911 beads were weighed and used in property measurements and ion exchange testing without modifications or washing.

Note that these two materials are identified in this report as "R9120-B" and "IE-911", but they are actually identical materials other than particle size and how the CST was pretreated with caustic.

[a] IONSIV is a trademark of Honeywell UOP, Inc. Des Plaines, Illinois, USA.

2.2 CST Physical Property Measurements for R9120-B

CST subsamples were characterized under nitrogen purge gas by Thermal Gravimetric Analysis (TGA) as described in earlier reports (King, et al., 2018a and 2018c). The particle size of the R9120-B media was measured using a Microtrac S3500 Laser Diffraction Analyzer. Samples were suspended in water for the analysis. Similar particle size analysis was conducted for IE-911 as reported previously (King, et al., 2018a). The CST supplier also provided sieve data.

The bulk density of a bed of R9120-B CST beads was measured by pouring a 31.5731 g sample of the pretreated material into a graduated cylinder (~0.94 inch inside diameter) and tapping the sides of the cylinder until a constant upper bed surface height was achieved. This formed a column of CST that was ~2 inches tall. The weight and volume of the packed bed were used to calculate the bulk density of the material. The exact volume of the final packed bed (26.1 mL) was determined by weighing an equivalent volume of water and calculating the bed volume using the density of water.

2.3 Computation of Particle Diameter Statistics Based on Sieve Analysis Data

Computation of an average spherically-equivalent particle diameter for the CST beads required generation of a cumulative distribution function based on the Rosin-Rammler fit (Table 2-1) for weight percent passing versus sieve size. The Rosin-Rammler equation is one of the most commonly used theoretical equations for fitting measured cumulative particle size distributions of crushed minerals and blastpiles (Latham, et al., 2002). Once the cumulative distribution function (cdf) was determined for each test sample, probability distribution functions (pdf) on a weight and number basis were computed. Given the pdf of the particle distribution on a number basis, the average spherically-equivalent diameter was computed based on nine distinct average diameter definitions over the wet sieve interval of interest. Nonlinear least squares optimization of the cost function computed from residuals of the sieve data and the Rosin-Rammler equation yielded characteristic size (x_c) and uniformity coefficients (m_{rr}), respectively. The Powder Technology Handbook (Gotoh, et al., 1997) provides nine distinct definitions of mean or average particle diameters.

Table 2-1. Rosin-Rammler Cumulative and Probability Distribution Functions.

Function	Basis	Equation
CDF	Weight	$W(x) = 1 - \exp\left\{-\left(x/x_c\right)^{m_{rr}}\right\}$
PDF	Weight	$\mathbf{W}(\boldsymbol{x}) = \frac{\boldsymbol{dW(x)}}{\boldsymbol{dx}} = \left(\frac{\boldsymbol{m_{rr}}}{\boldsymbol{x_c}}\right)\left(\frac{\boldsymbol{x}}{\boldsymbol{x_c}}\right)^{\boldsymbol{m_{rr}-1}} \boldsymbol{exp}\left\{-\left(\frac{\boldsymbol{x}}{\boldsymbol{x_c}}\right)^{\boldsymbol{m_{rr}}}\right\}$
PDF	Number	$n(x) = w(x)\big/ f(x)\sigma(x)x^3$

$W(x)$ = fraction by weight finer than a given sieve size or particle diameter
x = sieve size or particle diameter
x_c = Rosin-Rammler characteristic size, taken to be 63.2% passing size
m_{rr} = Rosin-Rammler uniformity coefficient
$f(x)$ = particle volume shape factor ($\pi/6$ for a sphere)
$\sigma(x)$ = particle density (assumed constant)

2.4 Simulant Preparation

A sample of tank waste simulant with the composition provided in Table 2-2 was prepared following the standard recipe [Walker, et al., 1999]. This aqueous simulant was developed to represent an Average SRS waste supernate liquid and this solution composition has been used in the past for ion exchange media performance evaluations. The simulant contains 5.6 M total Na^+, with anions dominated by nitrate, free hydroxide, and nitrite. After preparation, the simulant was filtered through a 0.45 µm polymer filter unit. The measured simulant density was 1.2508 g/mL at ambient temperature (20 °C). For comparison purposes, OLI's predicted simulant density was 1.2292 g/mL at 20 °C.

Table 2-2. SRS Average Simulant Composition Developed by Walker [1999].

Component	Molarity
Na^+	5.60
K^+	0.015
Cs^+	1.4 E-4
OH^-	1.91
NO_3^-	2.14
NO_2^-	0.52
AlO_2^-	0.31
CO_3^{2-}	0.16
SO_4^{2-}	0.15
Cl^-	0.025
F^-	0.032
PO_4^{3-}	0.01
$C_2O_4^{2-}$	0.008
SiO_3^{2-}	0.004
MoO_4^{2-}	0.0002

2.5 Batch Contact Test Equipment

Batch contact testing was performed by mixing the aqueous simulant with a small amount of CST in plastic bottles and agitating the samples in an Innova incubator shaker oven (Model 4230) for a period of time. Samples were agitated by orbital rotation at 150 revolutions per minute (RPM) and continuously maintained at a temperature of 23 °C.

2.6 CST Batch Contact Testing with SRS Average Simulant

Duplicate 10 mL sub-samples of the simulant solution (Table 2-2) were used for each batch contact test duration and mixed with separate ~0.1 g samples (reference state hydrated mass basis with no water content correction) of CST media. The simulant and CST test samples for each test duration were placed in separate 60 mL polyethylene bottles, transferred to the shaker oven, and continuously agitated. Additional replicate samples for the 1.0 hour contact were prewetted by overnight contact with SRS Average Simulant containing no added cesium to evaluate whether CST bead wetting effects influenced the cesium loading results during early contact times. Previous studies indicated wetting of the CST beads impacted the results for contact times <6 hours (King, 2018a). The oven temperature was set to 23 ºC and the temperature was recorded daily (excluding weekends). Analysis sub-samples from separate bottles were collected and filtered through 0.45 µm syringe filters after 1, 5.5, 24, and 48 hours of agitation with R9120-B media and

after 5.5 and 96 hours with IE-911 to determine the cesium loading versus time. Additional data at other contact times was collected in an identical manner with IE-911 media and reported separately (King, 2018a). Sub-samples were submitted for Cs^+ and Sr^{2+} analysis by Inductively Coupled Plasma – Mass Spectroscopy (ICP-MS). During testing, the temperature based on recorded data was 23.0 °C, except when the oven door was opened briefly during sample loading/unloading.

2.7 ZAM Isotherm Model Calculations

The ZAM Isotherm Model code is purchased commercial software developed at Texas A&M University by Rayford G. Anthony and Zhixin Zheng and designed to simulate ion-exchange equilibria of electrolytic solutions and CST solids. The ZAM code is a product of several years of development and research in Professor R. G. Anthony's Kinetics, Catalysis and Reaction Engineering Laboratory in the Department of Chemical Engineering at Texas A&M University. A description of the current ZAM model is available [Zheng, 1997].

Two types of ZAM Isotherm Model analyses were employed during this effort:

- Specific numerical batch contact calculations were performed to make direct comparisons between measured loadings and ZAM predicted values; and
- Series of calculations were conducted by varying the CsCl concentration (while maintaining charge balance) to map out a specific isotherm.

IE-911 and R9120-B are engineered forms of ion exchange media that are composed of the submicron-sized CST "powder" bound into an engineered bead with a binding agent. ZAM only calculates the CST media performance in its powdered form; therefore, to adjust for the engineered CST media, a fixed amount of engineered-form media must be mathematically converted into its powdered form (i.e., to maintain the actual amount of exchange sites present in each batch contact sample). Once the media is put into its equivalent powdered-form dry mass basis, ZAM calculations are performed. Upon completion of the ZAM batch contact calculations, the resulting ZAM loadings and distribution coefficients (K_d) values are then converted back to an engineered-form basis. All ZAM calculations were made using software version-4. Although version-5 was developed to improve the calculated competition between $SrOH^+$ and Cs^+, the outcome is identical to version-4 in SRS tank waste compositions and version-4 converges better than the later version-5. The ZAM model was developed based on batch contact data in the 25-44 °C range [Hamm, 2002]. ZAM input and output files for a subset of the batch contact cases considered are provided in Appendix A and Beta Values are provided in Appendix B. The Beta modeling parameter contains the ion selectivity coefficients making it dependent upon temperature and liquid composition.

The list of ionic species in the simulant shown in Table 2-2 had to be adjusted to achieve a more exact charge balance when performing ZAM isotherm and numerical batch contact calculations. As has been previously shown by SRNL, Cl^- is the best choice within the list of species to play as an ionic spectator for charge balancing (Hamm, et al., 2002; King, et al., 2018d). Thus, for ZAM predictions the charge balanced concentrations provided in Table 2-3 were employed.

In Table 2-3 only those species directly addressed within ZAM have non-zero concentration values and this included all major species (>0.01 M) present in the simulant. For specific ZAM cases, CsCl was added or removed to achieve a desired Cs^+ concentration level of interest.

Note: During document technical review, a small error (2.4%) in the measured water content of the CST was discovered which resulted in slightly lower amounts of CST in the batch contact tests on a dry mass basis than were assumed for the modeling evaluations. The corrected CST masses are provided in the report. However, since the reduced mass has a linear effect on the results and adjustments to the modeling results were expected to be minor, the decision was made not to recalculate the CST performance predictions.

Table 2-3. SRS Average Simulant Composition Charge Balanced for use in ZAM Predictions.

Component	Molarity
Na^+	5.60
K^+	0.015
Cs^+	1.45 E-4
OH^-	1.91
NO_3^-	2.14
NO_2^-	0.52
AlO_2^-	0.31
CO_3^{2-}	0.16
SO_4^{2-}	0.15
Cl^-	0.0530
F^-	0.032
PO_4^{3-}	0.01
$C_2O_4^{2-}$	0.0
SiO_3^{2-}	0.0
MoO_4^{2-}	0.0

3.0 Results and Discussion

3.1 Physical Property Measurements for R9120-B and IE-911 CST

The CST vendor supplied the following information on the sieve size analysis of this ion exchange media batch from the original manufacturing date:

Table 3-1. Vendor R9120-B Sieve Size Analysis Results

Screen cut	µm	wt %
(+18)	>1000	0.2
(18x20)	1000-841	4.6
(20x25)	841-707	12.3
(25x30)	707-595	18.3
(30x35)	595-500	33.7
(35x40)	500-420	25.3
(40x50)	420-297	4.4
(-50)	<297	1.3
	Sum =	100.1

SRNL computed the CST size characteristics from the vendor's sieve data as described in Section 2.3. Figure 3-1 shows a log-normal distribution fit of this sieve data. The log-normal distribution provides an adequate fit to this data when data uncertainty is considered.

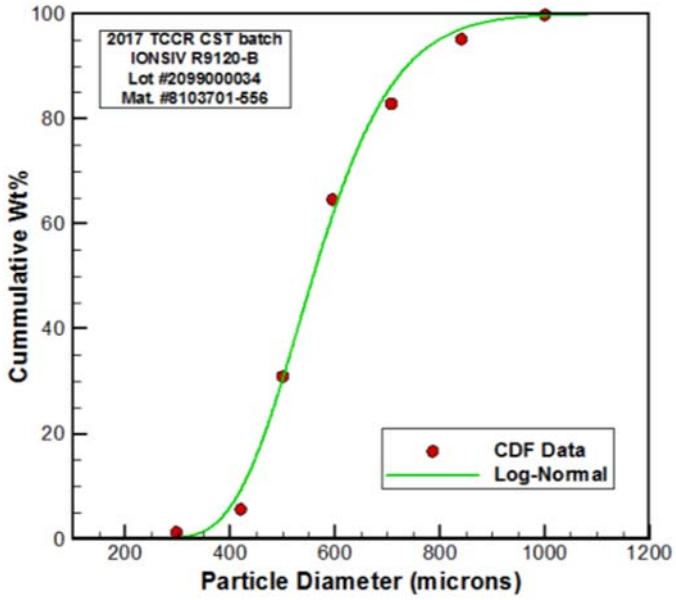

Figure 3-1. Computed Particle Diameter Fit to CST R9120-B Vendor Sieve Data.

From this Computed Diameter Fit (CDF) one can calculate a variety of different mean particle diameter sizes (i.e., most notable being the number, surface, and volume mean values). The volume mean value corresponds to the well-known "Sauter" mean diameter that historically has been preferred for addressing mass transfer from particles. The Sauter mean diameter represents the particle average value of volume per unit particle average value of surface area. The mean volume diameter for R9120-B is 572 microns. Table 3-2 contains the output from a calculational tool developed by SRNL (see Section 2.3), providing a variety of ways to express the particle size distribution for this CST batch. Residuals calculated as the difference between the measured and computed weight percent in each diameter range are provided the table. Two other methods of estimating the mean value of particle diameter are provided (i.e., number mean and surface mean).

Table 3-2. Computed Log-Normal Distribution of R9120-B Particle Size Based on Vendor Sieve Analysis.

Particle Size	Cumulative Distribution	Residual
(µm)	(wt % passing)	(obs-comp)
297	1.30	1.13
420	5.69	-3.62
500	30.97	0.629
595	64.64	3.20
707	82.92	-3.28
841	95.20	-1.88
1000	99.80	0.153
Log-Normal median size (xg) = 559 µm		
Log-Normal std deviation (sg) = 1.24		
Minimum particle size for integration = 200 µm		
Maximum particle size for integration = 1190 µm		
Number mean diameter = 497 µm		
Surface mean diameter = 546 µm		
Volume mean diameter = 572 µm		

The particle size of the pretreated sample of R9120-B was also measured using a laser diffraction analyzer (Microtrac S3500). Samples were suspended in water for the analysis. A single sub-sample was collected as a composite of beads from 4-5 different areas within the bottle, being careful to obtain representative subsamples. The results are shown in Figure 3-2 and Table 3-3. The average mean volume and area particle diameters for the sample were 566 and 480 µm, respectively. The volume-based mean particle diameter result by laser diffraction matches well with the average volume-based diameter (572 µm) computed from the sieve analysis results.

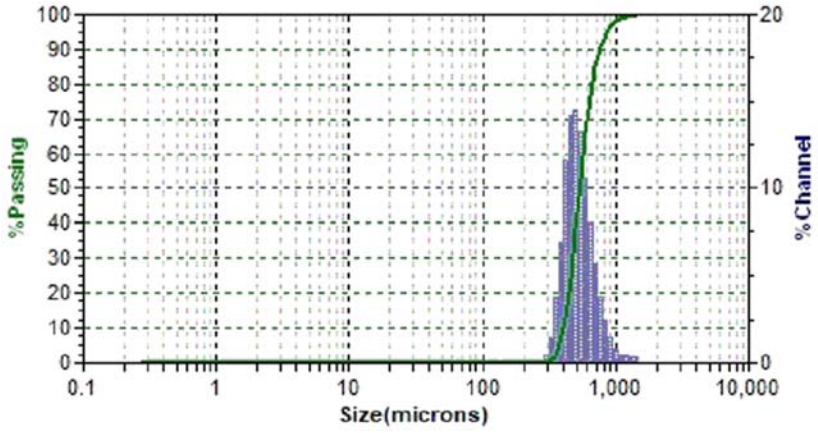

Figure 3-2. Microtrac Particle Size Analysis Results Plot for R9120-B CST Media.

Table 3-3. Microtrac Particle Size Analysis Data for R9120-B CST Media.

Data Item	Value
Mean Volume Diameter (μm)	566
Mean Number Diameter (μm)	480
Mean Area Diameter (μm)	531
Calculated Exterior Surface Area (m^2/mL)	1.13E-2

It was also important to visually examine the R9120-B material to see if there were any fractures, fines, or unusual particles and to determine the general particle shape. An optical microscope image of a R9120-B sub-sample is shown in Figure 3-3. There is no indication of significant bead fracturing or degradation in the sample. The CST beads are irregular in shape, but are generally round or elliptical. For comparison, a similar microscope image is provided for a sub-sample of IE-911 in Figure 3-4. Note that the magnification scales are not the same for the two images.

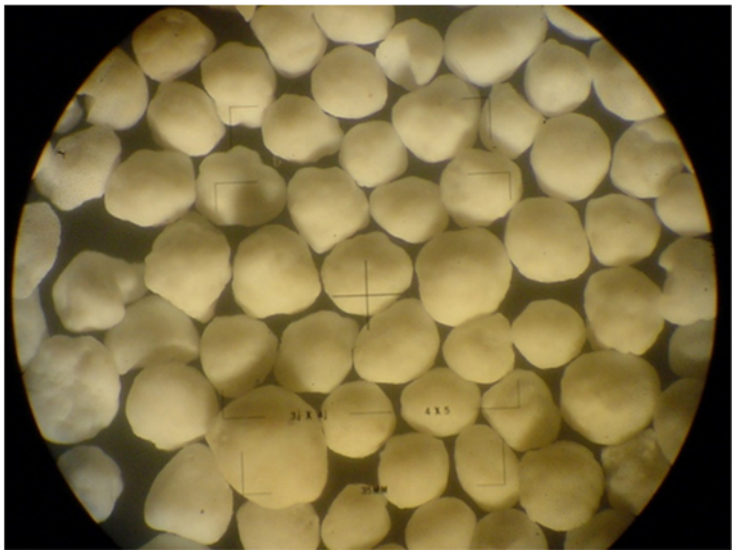

Figure 3-3. Optical Microscope Image of R9120-B CST Media.

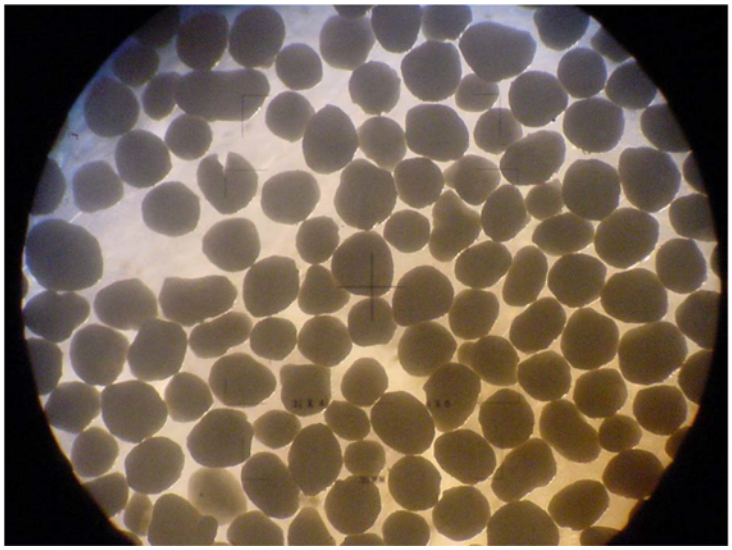

Figure 3-4. Optical Microscope Image of IE-911 CST Media.

Duplicate TGA results for the pretreated R9120-B and as-received IE-911 media used for this testing have been reported previously (King, et al., 2018a and 2018c). The cumulative percentages of both physisorbed and chemisorbed water in the samples was 18.2% and 16.3% for R9120-B and IE-911, respectively, based on heating to 400 °C in the TGA instrument. Conversion of the measured media reference state masses to a dry mass basis can be accomplished by multiplying the measured mass by factors (F-factors; dry mass correction factors) of 0.8177 (R9120-B) and 0.8374 (for IE-911). It should be noted that it is assumed that all mass losses from the media across this temperature range are associated with water loss, although the identity of the off-gas components was not confirmed by separate analysis.

The bulk density of a packed cylinder of the pretreated R9120-B material was determined to be 1.210 g/mL (standard reference state mass basis). The packed bed density is similar to, but slightly (3%) lower than, the value reported previously for IE-911 CST of 1.227 g/mL (King, et al., 2018a). The dry bed density for R9120-B after F-factor correction was 0.9892 g dry CST/mL, while the dry bed density for IE-911 was 1.028 g dry CST/mL.

CST vendor supplied sieve size data for IE-911 is provided in Table 3-4. This physical property data was also provided in an earlier report (King, et al., 2018a).

Table 3-4. Vendor R9120-B Sieve Size Analysis Results.

Screen cut	µm	wt %
(+30)	>595	2.7
(30x40)	595-420	37.3
(40x50)	420-297	53.4
(50x60)	297-250	6.0
(-60)	<250	0.5
Sum =		99.9

SRNL computed the CST size characteristics from the vendor's sieve data as described in Section 2.3. Figure 3-5 shows the log-normal distribution fit of this sieve data. Even though a course resolution of sieve data was taken, a very good fit was achieved. The mean volume diameter is 408 microns. Table 3-5 provides the output from the calculational tool developed by SRNL, providing a variety of ways to express the particle size distribution.

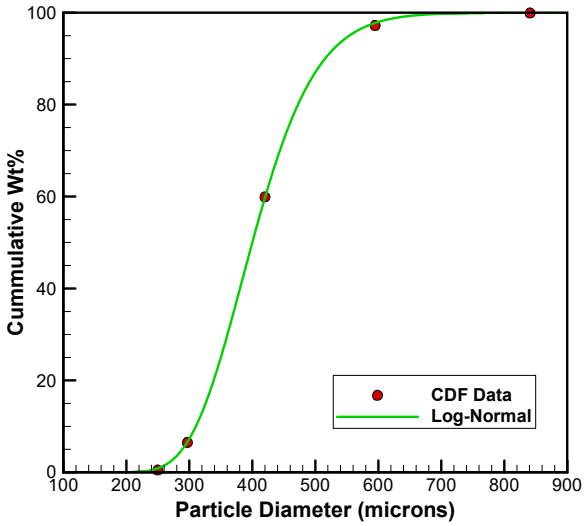

Figure 3-5. Computed Particle Diameter Fit to CST IE-911 Vendor Sieve Data

Table 3-5. Computed Log-Normal Distribution of IE-911 Particle Size Based on Vendor Sieve Analysis

Particle Size (µm)	Cumulative Distribution (weight % passing)	Residual (obs-comp)
250	0.50	-0.379
297	6.50	-0.130
420	59.90	0.144
595	97.20	-0.563
841	99.90	-0.0914
Log-Normal median size (xg) = 400 µm		
Log-Normal std deviation (sg) = 1.22		
Minimum particle size for integration = 210 µm		
Maximum particle size for integration = 1000 µm		
Number mean diameter = 363 µm		
Surface mean diameter = 392 µm		
Volume mean diameter = 408 µm		

3.2 CST Loading Batch Contact Kinetics Tests with SRS Average Simulant

Cesium loading batch contact kinetics tests were conducted at 23 °C using R9120-B and IE-911 CST media and SRS Average Simulant. Prior work indicated that cesium sorption to CST media from batch R9120-B is essentially complete within ~4 days with continuous and sufficient agitation [King, et al., 2018c]. Equilibrium cesium loading and distribution coefficients were calculated from measured initial and final cesium concentrations based on analytical results and sample masses. The equations employed are listed below:

$$\mathbf{K_d} = \left[\left(\frac{\mathbf{C_i}}{\mathbf{C_f}}\right) - \mathbf{1}\right]\left[\frac{\mathbf{V}}{\mathbf{mF}}\right] \quad (3\text{-}1)$$

where K_d - sorption phasic distribution coefficient, (ml/g) on a dry mass basis

C_i - initial liquid-phase Cs concentration, [M]

C_f - final (i.e., equilibrium) liquid-phase Cs concentration, [M]

V - liquid-phase volume, (ml)

m - CST in hydrated reference state mass, (g)

F - F-Factor for mass correction of CST water content,

The last grouping of terms in Eq. (3-1) is typically referred to as the phase ratio of a given batch contact experiment expressed as:

$$\boldsymbol{\phi} = \frac{\mathbf{V}}{\mathbf{mF}} \quad (3\text{-}2)$$

where ϕ - phase ratio, (ml/g) and usually stated on a dry mass basis

The Cs loading can then be computed from the above values by:

$$Q = K_d C_f \quad (3\text{-}3)$$

where Q - Total Cs loading on CST, (mmol/g) and usually stated on a dry mass basis

Loading also refers to form of CST being tested (i.e., either in powdered-form or engineered-form).

Batch contact slurries of simulant and CST beads (duplicate samples for R9120-B and individual samples for IE-911) were prepared for each time period to be measured, and the mixtures were removed from the shaker at the specified time, immediately filtered, and analyzed. Cesium loading kinetics sample data and analytical results are provided in Table 3-6. Comparison of results for pre-wetted and standard reference state samples (1 hour data in Table 3-6), indicates that pre-wetting the beads results in faster Cs^+ loading on CST within a 1 hour time frame (52.0% versus 46.8% Cs^+ removal on average). Therefore, the pre-wetted sample results are believed to be more representative of cesium loading kinetics behavior in a CST column immersed in waste supernate solution. The 1 hour data collected under normal batch contact conditions (no preliminary sample wetting using CST in the standard reference state) are believed to be biased low due to the impact of bead wetting effects during initial simulant contact. Analysis of the pre-wetting simulant indicated that the solution contained trace Cs^+. Based on the pre-wetting solution volumes, the amounts of Cs^+ in the pre-wetting solutions were <2% of the cesium in the batch contact test samples and the trace cesium ions present in the pre-wetting solutions are not expected to impact the cesium loading results significantly. Future kinetics testing should involve pre-wetting the CST samples for short duration simulant contacts. Cesium loading data versus time for the two CST media batches from this testing and earlier testing are plotted together in Figure 3-6 (% Cs^+ removal) and Figure 3-7 (Cs^+ mmol/g CST) for comparison.

Table 3-6. Cesium Loading Versus Time Test Results with TCCR Caustic-Washed R9120-B CST and SRS Average Simulant at 23 °C.

Sample	CST (g)	Simulant (g)	Initial Cs^+ (M)	Final Cs^+ (M)	K_d mL/g	% Cs^+ Removal	Cs^+ Loading (mmol/g)[a]
1.0 hour	0.1001	12.5105	1.45E-04	7.53E-05	---	48.2	8.57E-03
1.0 hour replicate	0.1003	12.5058		7.96E-05	---	45.3	8.03E-03
1.0 hour (pre-wetted)[b]	0.1000	12.5063		7.07E-05	---	51.4	9.14E-03
1.0 hour replicate (pre-wetted)[b]	0.1005	12.5066		6.90E-05	---	52.6	9.30E-03
5.5 hour	0.1002	12.5074		2.59E-05	---	82.2	1.46E-02
5.5 hour replicate	0.1003	12.5100		3.04E-05	---	79.1	1.40E-02
24 hour	0.1000	12.5027		1.63E-05	---	88.8	1.58E-02
24 hour replicate	0.1005	12.5071		1.43E-05	---	90.2	1.60E-02
96 hour	0.1000	12.5131		8.82E-06	1895	93.9	1.67E-02
96 hour replicate	0.1000	12.5097		9.22E-06	1806	93.7	1.67E-02

[a] dry CST mass basis
[b] CST pre-wetted by overnight contact in SRS Average Simulant containing no added Cs^+ salts

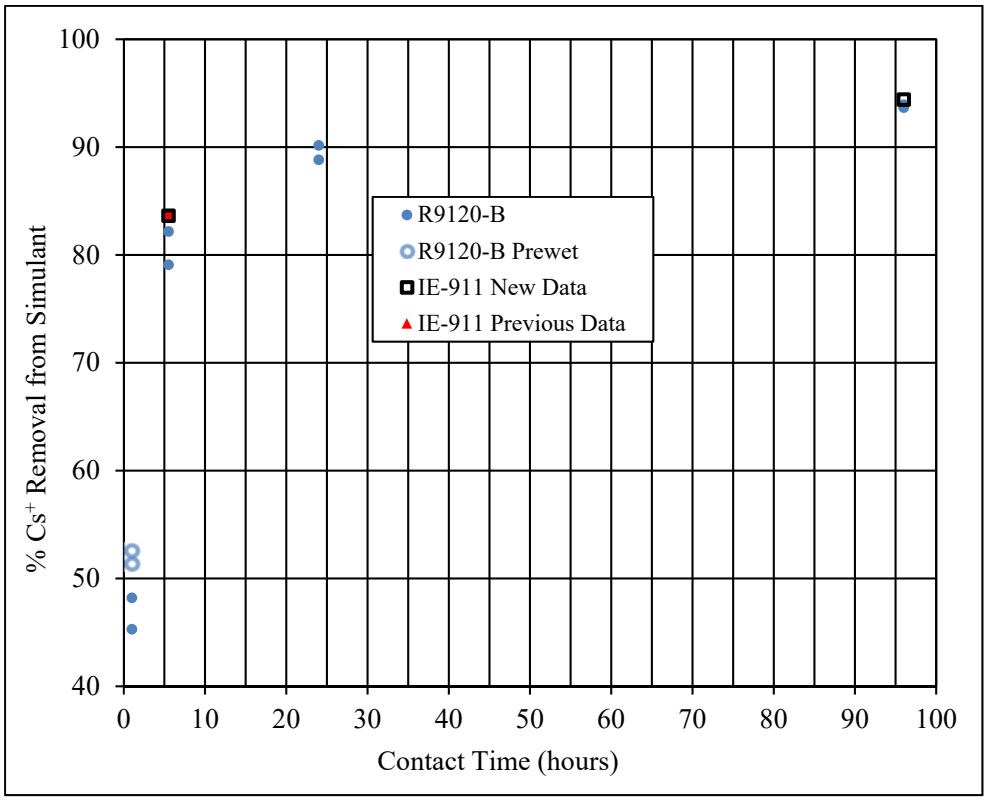

Figure 3-6. Cesium Percent Removal Versus Time for Caustic-Washed R9120-B and IE-911 Media with SRS Average Simulant at 23 ºC.

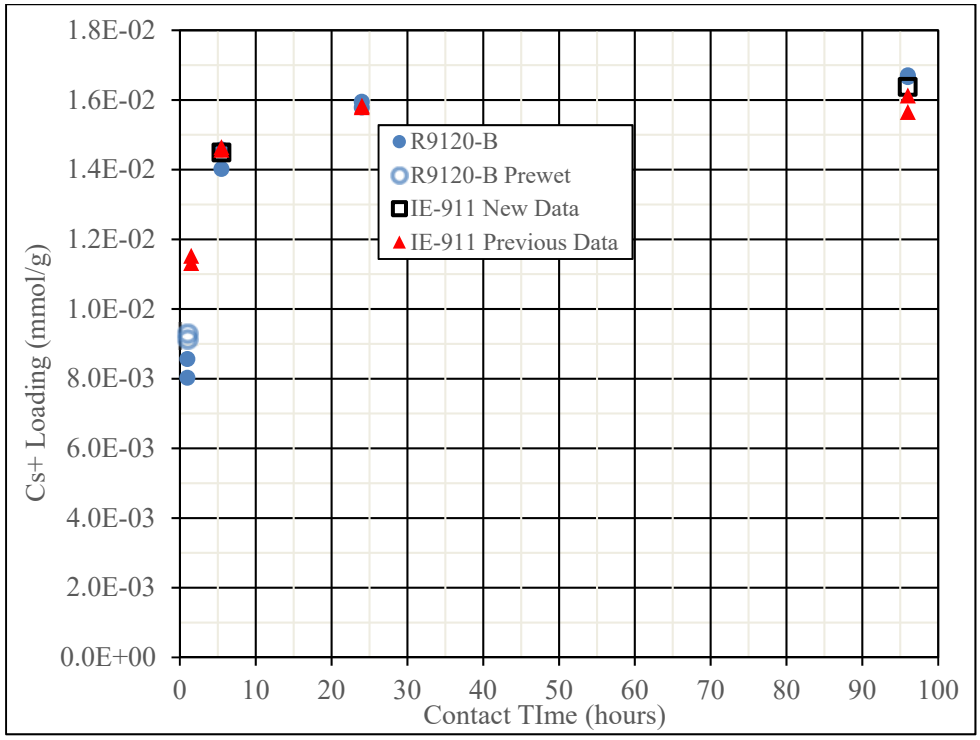

Figure 3-7. Cesium Loading on Solid Phase (dry CST basis) Versus Time from SRS Average Simulant on CST at 23 °C.

Strontium analysis results for the solutions (feed and batch contact filtrates) are provided in Table 3-7. Detectable strontium was present in the simulant solutions as a reagent impurity at low concentrations and strontium was adsorbed from the solutions by the CST (final concentrations ≤1.14E-8 M). Although strontium, as the $SrOH^+$ ion, is a very strong competitor for ion exchange sites on CST, the initial molar strontium concentration (5E-7 M) in this simulant is 6% of the lowest final Cs^+ concentration (8E-6 M) observed, so its effect would not measurably influence the Cs^+ loading.

Table 3-7. Strontium Analysis Results for Feed and Batch Contact Solutions.

Sample	Initial Sr^{2+} (M)	Final Sr^{2+} (M)
1.0 hour	4.93E-07	1.96E-07
1.0 hour replicate		1.88E-07
1.0 hour (pre-soaked)		1.49E-07
1.0 hour replicate (pre-soaked)		1.64E-07
5.5 hour		3.48E-08
5.5 hour replicate		3.12E-08
24 hour		1.87E-08
24 hour replicate		1.70E-08
96 hour		<1.14E-08
96 hour replicate		<1.14E-08

3.3 Test Result Comparisons with Modeling

Computational data evaluations and predictions are provided and discussed in detail in the Appendices.

Note: During document technical review, a small error (2.4%) in the measured water content of the CST was discovered which resulted in slightly lower amounts of CST in the batch contact tests on a dry mass basis than were assumed for the modeling evaluations. The corrected CST masses are provided in the report. However, since the reduced mass has a linear effect on the results and adjustments to the modeling results were expected to be minor, the decision was made not to recalculate the CST performance predictions.

Calculated CST equilibrium isotherm comparisons to experimental batch contact data are provided in Figure 3-8. More detailed information on ZAM modeling comparisons to the data is provided in Appendix A. A binder dilution factor (BDF) of 0.76 was used to match the equilibrium cesium loading, which is a slightly smaller mass correction than was used in recent testing (BDF = 0.68; King, et al. 2018c). Very similar overall behavior was observed for the IE-911 CST reported by King, et al., 2018a, with the primary difference being that the binder dilution factor for the IE-911 CST was 0.95.

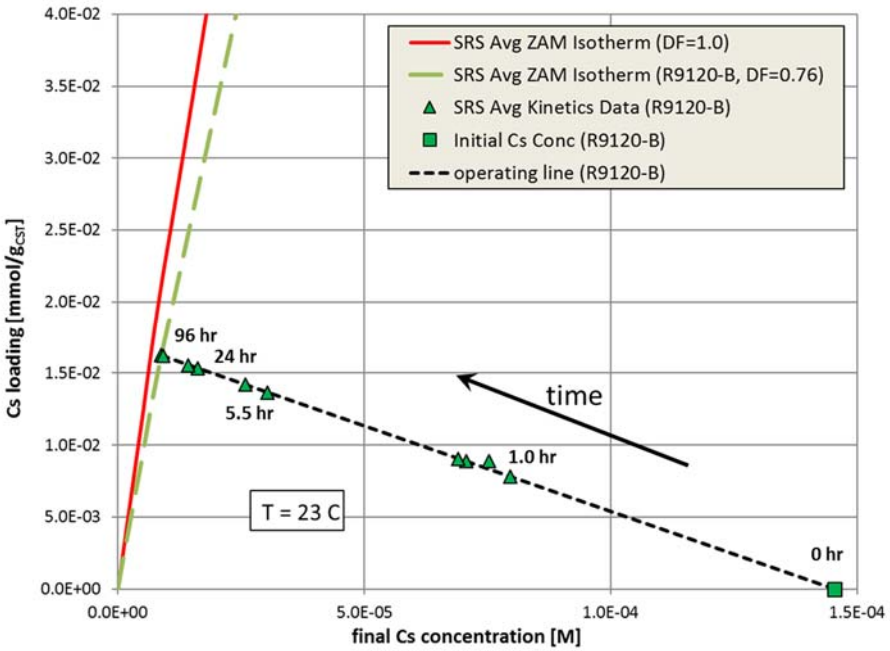

Figure 3-8. Approach, along an operating line, to equilibrium for the R9120-B engineered-form CST media in contact with SRS Average Simulant at 23 °C.

Cesium loading kinetic data evaluations versus the τ model input value are provided in Figure 3-9. More detailed information on VERSE modeling evaluations of the batch contact kinetics data is provided in Appendix B. The τ value represents the inverse of the cesium diffusivity expressed as a fraction of the free stream diffusivity. For instance, a τ of 4 is ¼ of the cesium free stream diffusivity. To determine τ, the VERSE column model was manipulated into mimicking a static system, using a column configuration with minimal liquid flow and disabling the film diffusion coefficient. As shown in Figure 3-9, the batch contact kinetics data exhibited larger data variability at shorter contact times. This is probably due to increased sensitivity at the higher cesium transfer rates (liquid to solid) occurring at shorter times. As mentioned previously, inadequate particle wetting effects are also observed when pre-wetting steps are not employed. VERSE predictions did not capture the early time data even when attempts to pre-wet the material were implemented. It is speculated that at these early times, agitation rates were insufficient to maintain adequate film diffusion coefficients. If shorter contact times are evaluated in future kinetics testing, both particle pre-wetting techniques and more effective solid-liquid contact methods should be utilized. As expected, the overall response is faster for the smaller IE-911 material due to the smaller particle size. Two different tortuosity factor values were considered (i.e., 4.0 and 5.0). A tortuosity factor of 4.0 fits the IE-911 data well, while a value slightly higher, around 4.5 might be a better fit to the R9120-B. It should be emphasized that VERSE only represents the distribution of particles being tested by a single average particle size and this assumption could yield a systematic bias within the predictions.

As shown in Appendix B, separate evaluations revealed that the actual numerical value of the tortuosity factor is dependent upon what specific particle size metric is chosen. A simple correlation between tortuosity factor and particle size exists for CST media. For the purposes of this report, the volume mean average (i.e., Sauter mean) particle size metric was chosen. This is

the metric generally preferred when computing mass transfer in packed beds. We recommend sieve data and the Sauter mean metric as the standard protocol for the average particle diameter.

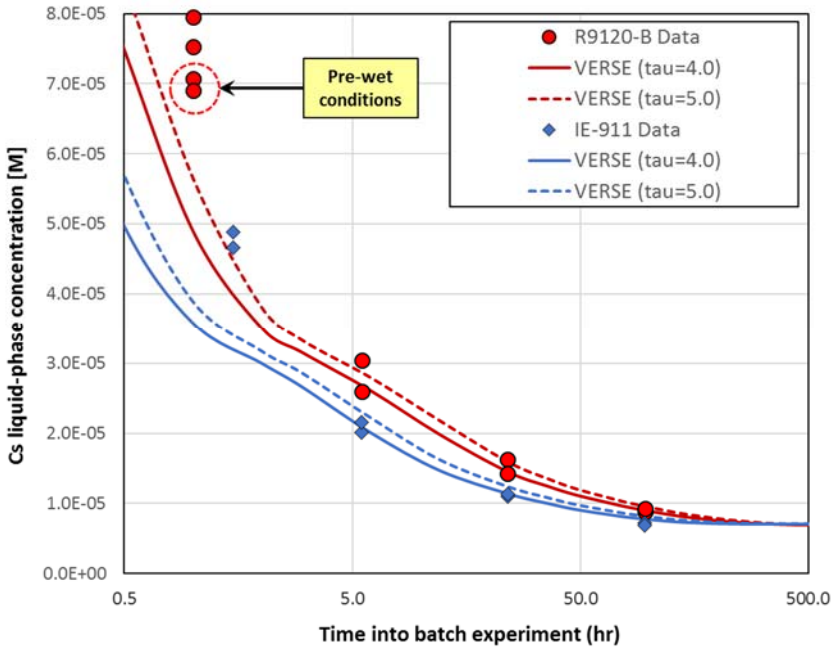

Figure 3-9. CST (IE-911 and R9120-B) particle kinetic data versus VERSE modeling highlighting impact on particle size and batch differences.

Calculated cesium breakthrough profiles are provided in Figure 3-10 for planned experimental conditions (single laboratory scale columns, 3 BV/hr flowrate, 23 ºC, $\tau = 4.0$) where it is apparent that significantly faster breakthrough is expected for the R9120-B CST. More detailed discussion of the VERSE calculations is provided in Appendix C. The calculations are based on a single 24 mL column case, while TCCR operations are expected to involve at least two larger (~132 gallons) columns in series. For the single laboratory column operation, approximately 2.5 times more waste simulant volume can be processed with IE-911 CST than with the R9120-B media at a flow rate of 3 column bed volumes per hour (BV/hr) when targeting a cesium decontamination factor of

1000 (instantaneous breakthrough basis). For TCCR multiple column operations, the impact of the CST batch will be lower than predicted for the single column case.

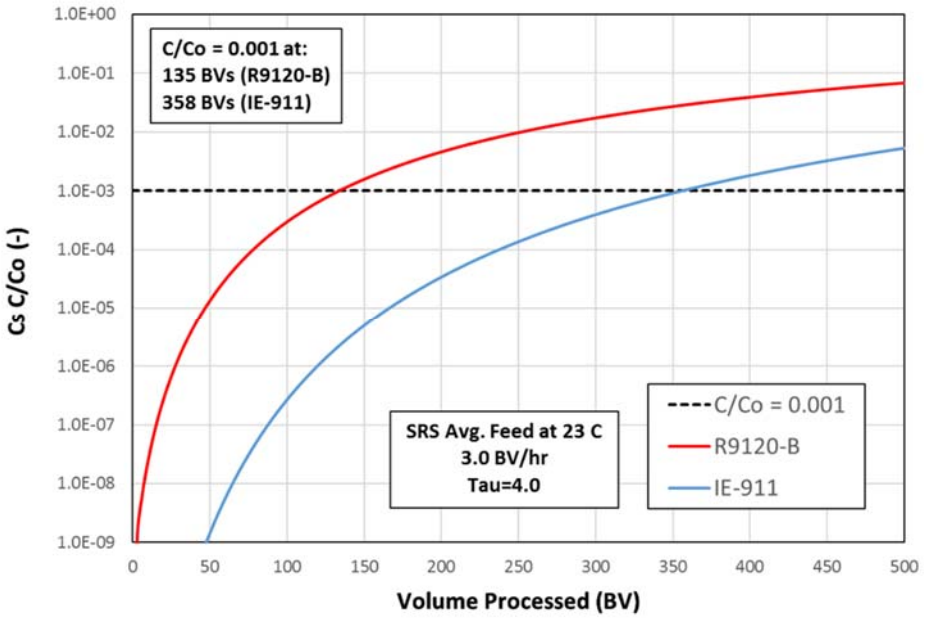

Figure 3-10. VERSE predicted basecase Cs breakthrough curves based on single columns using IE-911 and R9120-B CST materials with SRS Average Simulant feed at 23°C (semi-log plot).

Waste volume processing rate effects on cesium breakthrough profiles for the single laboratory columns with R9120-B CST were also calculated using the VERSE model as shown in Figure 3-11, where it is apparent that decreasing the flow rate from 6 to 1 BV/hr results in a large increase (~6.5x) in volume processed before reaching the target DF. Slower waste processing flow rates can obviously be used to compensate for the impact of larger particle diameter in R9120-B CST.

As shown in Appendix C, other analysis indicated that temperature effects on column performance had minimal influence on waste volume processed to reach the DF across the range of 23-40 °C. Column performance sensitivity studies were also conducted for the tortuosity factor parameter and correlations between the tortuosity factor and the particle size metric selected were determined.

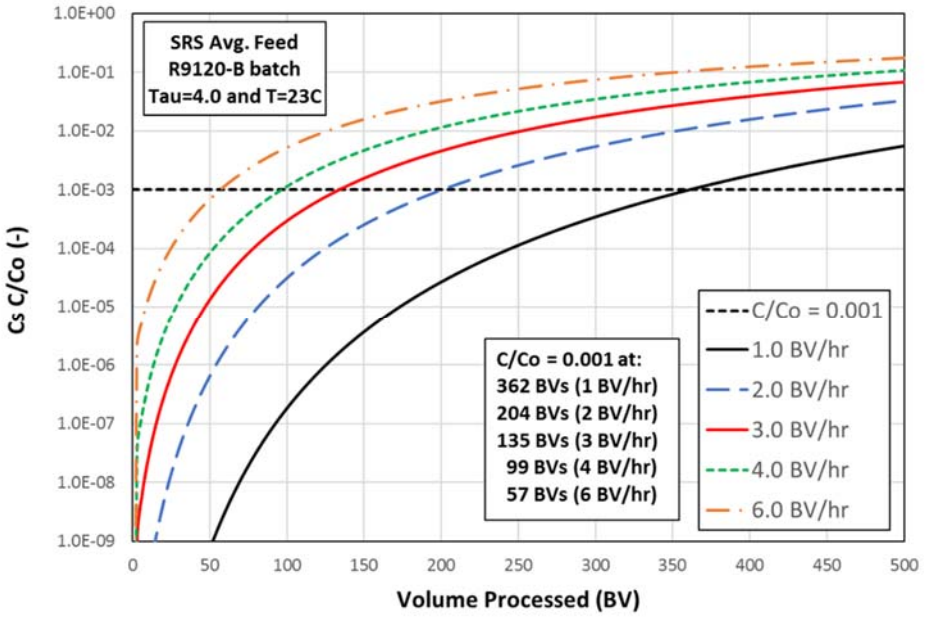

Figure 3-11. VERSE predicted flowrate impact on Cs breakthrough curves based on single columns using R9120-B CST material with SRS Average Simulant feed at 23°C (semi-log plot).

4.0 Conclusions

Cesium loading data and modeling evaluations confirmed that the R9120-B CST ion exchange media batch planned for use in the TCCR columns is pore diffusion limited (cesium loading rates limited by intraparticle diffusion) with a similar tortuosity factor ($\tau = 4$) to earlier IE-911 CST batches. The larger average particle diameter for R9120-B CST leads to slower cesium uptake rates for this media batch. As a result, significantly earlier cesium breakthrough is expected during column operations with R9120-B CST versus IE-911. For example, when processing SRS Average Simulant at 23 °C through a single CST column at 3 BV/hr, the effluent solution is expected to reach a cesium decontamination factor of 1000 after processing approximately 40% of the volume that could be processed prior to reaching this limit with IE-911 CST. A smaller difference in volume processed would be observed when operating in a lead/lag column configuration as was done with TCCR. To mitigate the adverse influence of the larger particle size, a slower flow rate would allow processing of larger volumes. For example, varying the column processing flow rate for R9120-B CST from 6 to 1 BV/hr. in the single column configuration case results in a 6.5x increase in volume processed before reaching the target DF of 1000. Other analysis indicated that temperature effects on column performance had minimal influence on waste volume processed to reach a DF of 1000 across the range from 23-40 °C. Column performance sensitivity studies were also conducted for the tortuosity factor parameter, and correlations between the tortuosity factor and the particle size metric selected were identified.

5.0 Recommendations

Resolution is needed regarding the apparent inconsistency in "dilution factor" from the CST binder; i.e., variability in adjusting the ZAM modeling to match the test results. Since recent evaluations have involved consistent preconditioning, drying, F-factor, and test procedures and some variability has still been observed (0.68 to 0.76 for R9120-B) it appears possible that analytical variability might be a contributor. Future studies should consider the use of a cesium standard of known concentration to evaluate this possibility.

We recommend sieve data and the Sauter mean metric as the standard protocol for the average particle diameter.

It would be useful to establish a standard protocol to check the kinetics of CST batches so that the kinetics performance can be evaluated without performing column tests. This would include pre-wetting the CST media so that pore diffusivity is not impacted by using dry material and using greater agitation rates for short term contacts.

Consistent preparation and use of simulants are recommended. Standard practice should include the measurement of all competing species (i.e. strontium) in tank waste samples and those present as impurities in the simulants used for any testing.

Side-by-side column tests with the two media batches under identical conditions are recommended since this is the best and preferred method of performance comparison. Evaluations of processing outage scenarios where flow is stopped (as occurred during TCCR processing) should also be conducted.

6.0 References

Beasley, M.H., Coleman, A.D., Croy, B.H., Fink, S.D., Jacobs, R.A., and Walker, D.D., 2000. "IONSIV® IE-911 Performance in Savannah River Site Radioactive Waste", WSRC-TR-2000-0052.

Choi, A. S., 2001. "Software Quality Assurance Plan for Hanford RPP-WTP Evaporator Modeling (U)", WSRC-RP-2001-00337, Rev. 0.

Duffey, C. E., King, W. D., Hamm, L.L., 2002 . "Determination of Perrhenate (ReO_4^-) Adsorption Kinetics from Hanford Waste Simulants Using SuperLig® 639 Resin", WSRC-TR-2002-00548, Rev. 0.

T. L. Fellinger, 2018. "Tank Closure Cesium Removal (TCCR) Project - Tank 10H Radioactive Batch Contact Tests", X-TTR-H-00072, Rev. 1.

Gotoh, K., Masuda, H., Higashitani, K., Powder Technology Handbook, 2nd Revision Edition, Marcel Dekker, New York, 1997.

Hamm, L. L., F. G. Smith, and M. A. Shadday, 1999. "QA Verification Package for VERSE-LC Version 7.80," WSRC-TR-99-00238, Rev. 0.

Hamm, L. L., T. Hang, D. J. McCabe, and W. D. King, 2001. "Preliminary Ion Exchange Modeling for Removal of Cesium from Hanford Waste Using Hydrous Crystalline Silicotitanate Material", WSRC-TR-2001-00400, Rev. 0.

Hamm, L. L., Hang, T., McCabe, D. J., King, W. D., 2002. "Preliminary Ion Exchange Modeling for Removal of Cesium from Hanford Waste Using Hydrous Crystalline Silicotitanate Material", WSRC- TR-2001-00400, SRT-RPP-2001-00134, Rev. 0.

Hamm, L. L., McCabe, D. J., 2018. "Crystalline Silicotitanate Ion Exchange Column Sizing and Sensitivity Study in Support of the Hanford Test Bed Initiative", SRNL-STI-2018-00513, Rev. 0.

Hang, T., 2017. "Software Classification Document – VERSE-LC," G-SWCD-A-00060, Rev. 0.

King, W. D., McCabe, D. J., Hamm, L. L., Nash, C. A., Fondeur, F. F., 2018a. "Crystalline Silicotitanate Ion Exchange Media Long-Term Storage Evaluation", SRNL-STI-2018-00567, Revision 0.

King, W.D., 2018b. "Task Technical and Quality Assurance Plan for Batch Contact Sorption and Desorption Testing to Support Tank Closure Cesium Removal Operations", SRNL-RP-2017-00536, Rev. 1.

King, W. D., Hamm, L. L., Coleman, C. J., Fondeur, F. F., Reboul, S. H., 2018c. Crystalline Silicotitanate (CST) Ion Exchange Media Performance Evaluations in SRS Average Supernate Simulant and Tank 10H Waste Solution to Support TCCR, SRNL-STI-2018-00277, Revision 0.

King, W. D., Hamm, L. L., Nash, C. A., Fondeur, F. F., McCabe, D. J., 2018d. "Test Matrix to Evaluate Anion Effects on CST Loading for TCCR", SRNL-L3100-2017-00104, Rev. 0.

Latham, J. P., Munjiza, A., Lu, Y., "On the Prediction of Void Porosity and Packing of Rock Particulates", Powder Technology, 2002, Vol. 125 pp. 10-27.

Tamburello, D. A., 2011. "Software Classification Document – ZAM," B-SWCD-A-00598, Rev. 0.

Walker, D.D., 1999. "Preparation of Simulated Waste Solutions", WSRC-TR-99-001 16, Rev. 0.

Zheng, Z., Anthony, R. G., and J. E. Miller, 1997. "Modeling Multicomponent Ion Exchange Equilibrium Utilizing Hydrous Crystalline Silicotitanates by a Multiple Interactive Ion Exchange Site Model," Ind. Eng. Chem. Res., Vol. 36, No. 6, pp. 2427-2434.

Appendix A. CST Isotherm Analyses using ZAM

In this appendix the aspects of CST Cs isotherms are discussed. Both powdered-form and engineered-form(s) CST media are considered where the focus is on their loading behavior when in contact with SRS Avg simulant.

A.1 CST Powdered-form Cs Isotherm for SRS Average Simulant

As discussed in Hamm et al. (2002) a binary Cs CST isotherm can be created using the ZAM code for a specific chemical composition. This is accomplished by performing a series of ZAM calculations at a fixed temperature where the liquid-phase composition is varied by addition of varying amounts of CsCl (i.e., all other cations and anions being held fixed). Typically, the Cs^+ concentration is varied from $1.0x10^{-9}$ M up to $1.0x10^{-1}$ M using one order of magnitude increases. Thus, nine separate ZAM numerical batch contact calculations are performed where the phase ratio employed is sufficiently large (much greater than 100 in most cases) that the liquid phase cesium concentration change associated with ion exchange is negligible. For the SRS Average Simulant as compositionally provided in Table 2-3 and at a solution temperature of 23 °C the predicted Cs loading values for CST in its powdered-form are shown in Figure A-1.

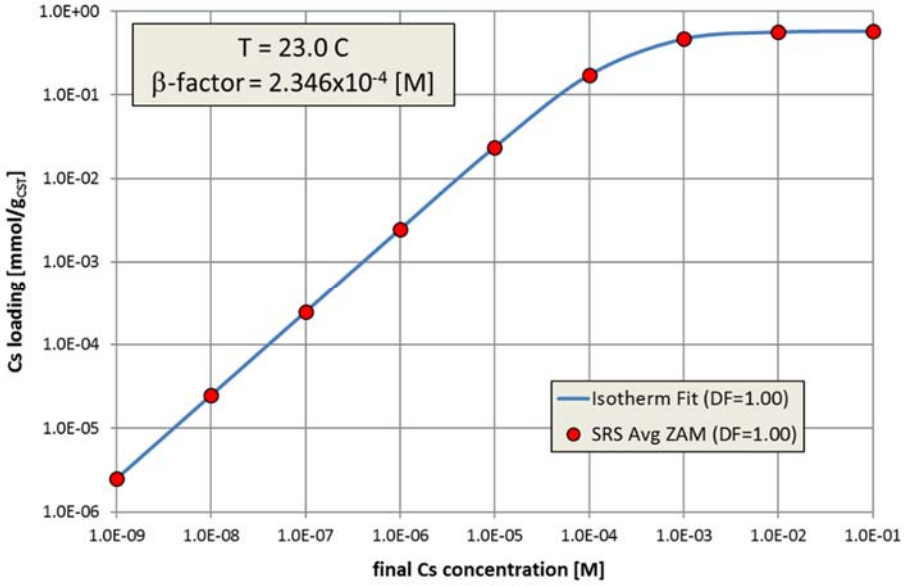

Figure A-1. ZAM based binary Cs^+ isotherm for SRS Average Simulant at 23°C and CST in its powdered-form (IE-910).

In numerous prior SRNL efforts it has been verified that the ZAM predicted binary Cs isotherm can be very effectively expressed by a binary Langmuir isotherm as expressed by:

$$Q_{Cs} = \frac{\eta Q_T c_{Cs}}{c_{Cs} + \beta(T)} \qquad \text{(A-1)}$$

where Q_{Cs} - total Cs loading, (mmol/g) on a dry CST mass basis

c_{Cs} - liquid-phase Cs concentration, [M]

Q_T - total Cs ionic exchange capacity, (0.58 mmol/g) on a dry CST mass basis

β - temperature dependent beta-factor, [M]

η - CST-form dependent binder dilution-factor (BDF),

T - system temperature, (°C)

The binder dilution factor in Eq. (A-1) becomes unity when viewing powdered-form results and generally becomes less than unity when engineered-forms are being considered (e.g., see Hamm et al., 2002).

In Figure A-1 the red circles represent the nine individual ZAM calculations that represent the predicted Cs loadings on the CST powdered-form media for the SRS Average Simulant at 23°C. The solid blue curve represents a fit to the ZAM results based on Eq. (A-1). A single constant beta-factor value was obtained that yields a very good fit to the entire range of Cs concentrations and chemical compositions shown. At 23 °C this constant beta-factor takes the value:

$$\beta(23°C) = 2.346x10^{-4}\,[M] \qquad \text{(A-2)}$$

there the BDF was set to 1.0.

The CST powdered-form Cs isotherm is considered batch independent. Batch dependency only enters the isotherm through the BDF value. For future experiments where the operating temperature might be varied from the 23°C value, beta-values over a range of temperature were considered (i.e., 10 °C to 45 °C by 5 °C increments). The results of these analyses are shown as red circles in Figure A-2.

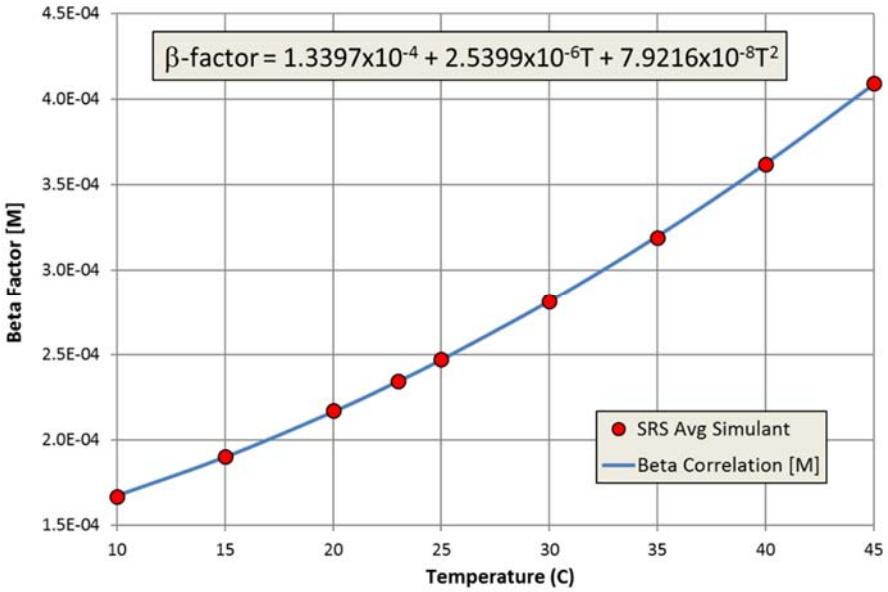

Figure A-2. Temperature dependent beta-factor for binary Cs^+ isotherm for SRS Average Simulant and CST in its powdered-form (IE-910).

The computed beta-factors were also fitted to the following quadratic polynomial:

$$\beta(T\,in\,°C) = 1.3397x10^{-4} + 2.5399x10^{-6}T + 7.9216x10^{-8}T^2\,[M] \qquad \text{(A-3)}$$

Equation (A-3) is shown in Figure A-2 as the solid blue curve.

A.2 CST Engineered-form Cs Isotherm for SRS Average Simulant

Over time batch contact testing has been performed using engineered-forms of CST media in contact with SRS Average Simulant. These tests have been employed as benchmarking studies by SRNL. The batch contact testing was performed where controlled agitation was maintained throughout the contact period and generally equilibrium was believed to have been achieved within 96 hours.

Historically, binder dilution factors less than unity were observed; however, in a few cases BDF values close to unity were measured (i.e., even values slightly larger than unity). This variability is now believed to be primarily the result of variations in the reference state of the CST media prior to the actual batch contact because the caustic-washing and the need for conversion entirely to Na-phase was not fully understood until approximately 2001. No details in the literature can be found associated with ZAM's (created at Texas A&M) dry mass reference state. The total Cs ionic exchange capacity employed within ZAM was provided by Zheng et al. (1997) and in several other Zheng reports as 0.58 mmol/g of CST media. Unfortunately, no details as to the actual protocol employed was provided.

To see the variations in engineered-form CST isotherms, four separate sets of CST batch contact data are compared to ZAM based Cs isotherms in Figure A-3.

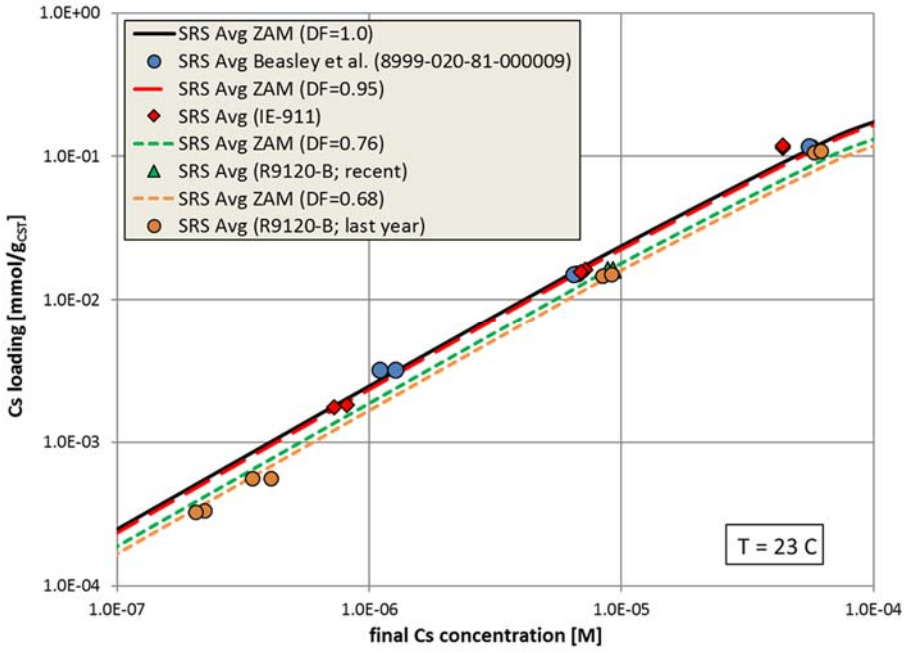

Figure A-3. Comparison of equilibrium batch contact data versus ZAM predictions for various engineered-form CST media in contact with SRS Avg simulant at 23 °C.

In Figure A-3 equilibrium batch contact data for three different engineered-forms of CST media are shown:

- **Blue circles** – data from Beasley et al. (2000) for IE-911 batch 8999-020-81-000009. The data suggested a BDF of about 1.0.
- **Red diamonds** – data from this report and a previous report (King, 2018a) for the ~17 year old CST media (IE-911 batch). The lower two data pairs indicated a BDF of about 0.95.

At higher Cs^+ concentrations, BDF values greater than unity have been observed on several occasions.

- **Green triangles** – data from this report for the current CST media being employed in the TCCR columns (R9120-B). A BDF of about 0.76 is indicated.
- **Orange circles** – data from last year in King et al. (2018c) for the current CST media being employed in the TCCR columns (R9120-B). The lower three data pairs indicated a BDF of about 0.68. Here again the upper data pair suggests a higher BDF value around 0.90 applies.

A.3 Approach to Equilibrium with Short Batch Contact Times

Batch contact testing was performed for both the IE-911 and R9120-B CST batches. The same SRS Average Simulant was used at 23 °C. Essentially, the batch contact tests were all performed as close to identical cases as possible (e.g., same phase ratios, initial Cs concentrations, etc.).

For the IE-911 batch a comparison of the batch contact data is shown in Figure A-4 along with the ZAM generated powdered-form isotherm and the estimated engineered-form IE-911 isotherm (based on the near equilibrium batch contact results).

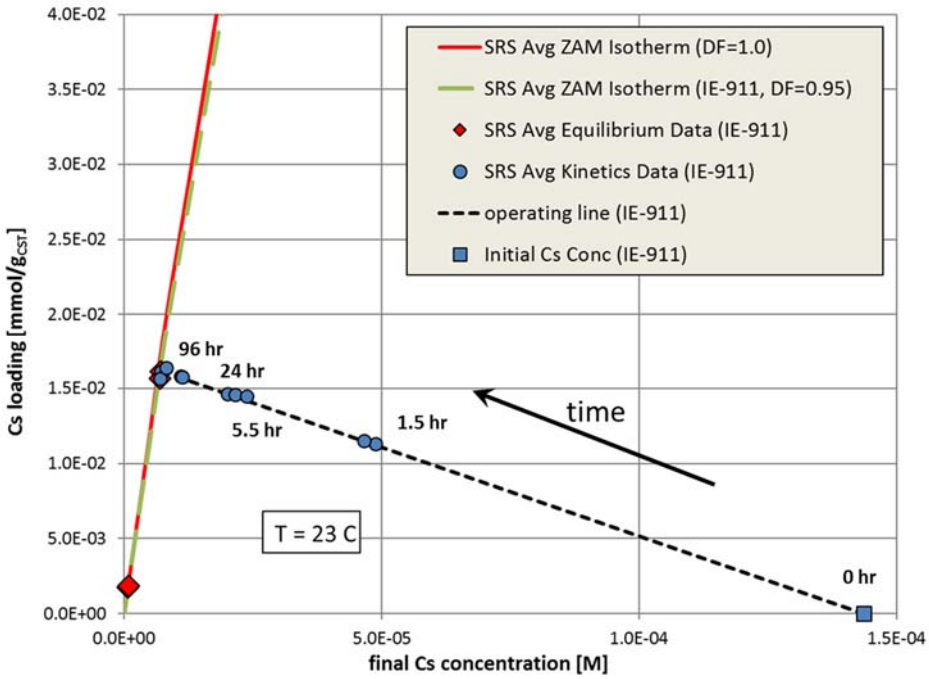

Figure A-4. Approach, along an operating line, to equilibrium for the IE-911 engineered-form CST media in contact with SRS Average Simulant at 23 °C.

The IE-911 equilibrium batch contact data is provided as red diamonds while the shorter timed batch contact data is provided as blue circles. The initial condition is shown as a blue square where fresh CST material was employed. The black dashed line represents the effective operating line (i.e., the basic mass balance for Cs between the liquid and solid phases). At the point of 96 hours of contact the last pair of batch contact data is consistent with the estimated isotherm represented as a long-dashed curve in light green. The slight deviations of the blue circles from the operating line reflects the slight variations in phase ratio observed among the various batch contact tests.

Very similar overall behavior is observed for the data shown in Figure A-5 for the newer CST media R9120-B. The main difference between these two sets of data regarding equilibrium behavior is:

- IE-911 – BDF = 0.95
- R9120-B – BDF = 0.76

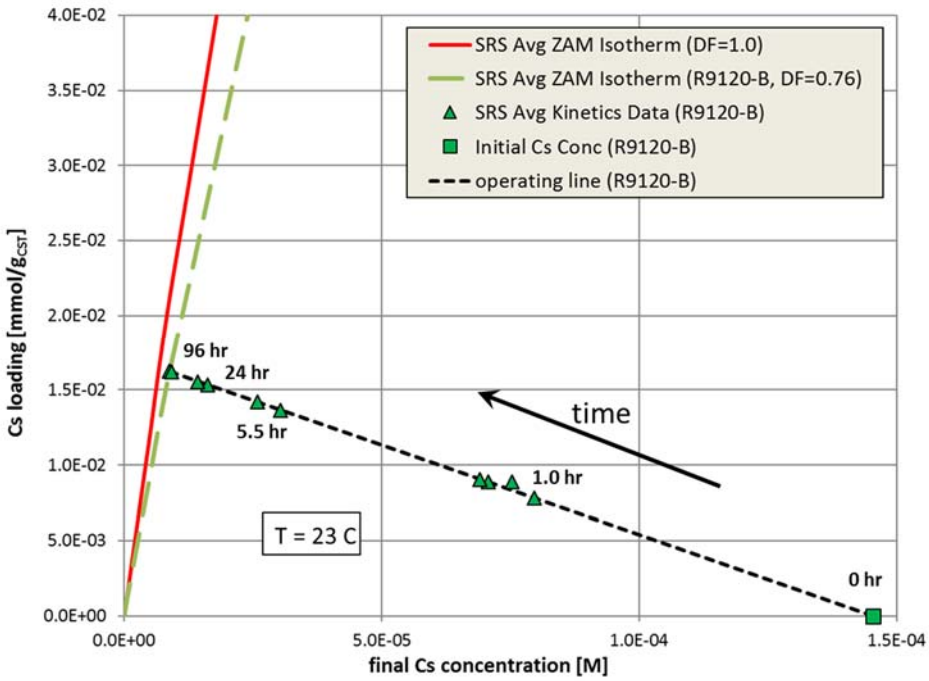

Figure A-5. Approach, along an operating line, to equilibrium for the R9120-B engineered-form CST media in contact with SRS Average Simulant at 23 °C.

Appendix B. CST Particle Kinetics

Figure B-1 illustrates the various mass transfer mechanisms occurring in a cartoon fashion for a fixed column of CST particles with liquid feed flowing through the bed where local mass transfer of Cs ions into the particles is occurring. Specifically, the key mass transfer mechanisms are:

- Bulk (bed) advection
- Film Diffusion
- Pore Diffusion
- Surface Ion Exchange

At a local particle the last three mechanisms above are occurring where it is generally assumed that the surface exchange is very fast and never limits the process. Therefore, only film and pore diffusion must be addressed. Since kinetics is a local phenomenon batch contact testing is an option.

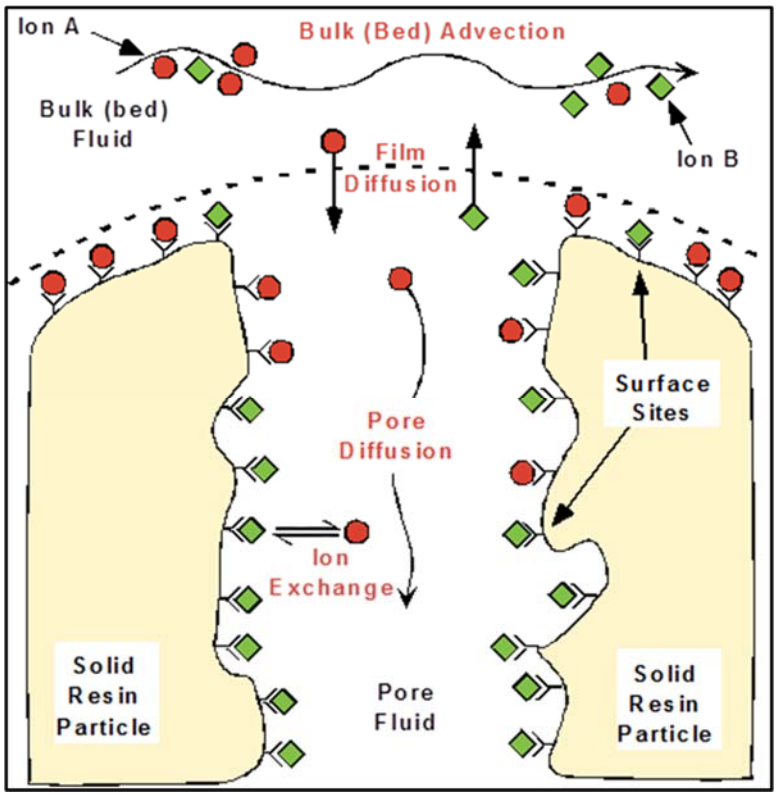

Figure B-1. Cartoon illustrating the various mass transfer mechanisms occurring at a specific CST particle.

Batch contact testing is straightforward as illustrated in Figure B-2. The desired goal of a batch contact test is isolation of the pore diffusion aspect from the film diffusion that occurs along the outer surface of CST particles. The degree of adequate controlled agitation is dependent upon the mass transfer response and this issue will be discussed below.

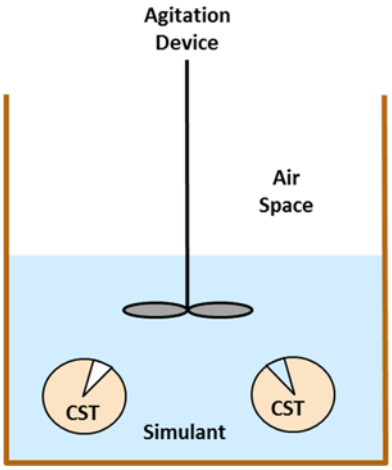

Figure B-2. Cartoon illustrating the basic elements of a batch contact test.

To model the kinetic behavior occurring within the CST particles the VERSE code was chosen. The details on how to construct a VERSE model for simulating behavior during the kinetic portion of a specific batch contact test are provided in Hamm et al. (2002).

The equilibrium isotherms employed within the VERSE simulations are provided in Appendix A for both the IE-911 and R9120-B CST batches considered. The batch kinetic testing was done using the SRS Average Simulant at 23 °C.

B.1 Kinetics Testing using the Batch Contact Method

One method of investigating CST particle kinetics is making use of a series of batch contact tests where a known and constant amount of CST material is placed in contact with a known and constant amount of simulant. Sufficient agitation must be employed to ensure that Cs^+ mass transfer is limited only by pore diffusion. The batch contact tests can involve differing amounts of contact time. Typically, the two end point contact times are:

- **Short contact timing** – Ideal for the initial rapid response in mass transfer but difficult to ensure that initial conditions are correct and that only limited by pore diffusion.
- **Long contact timing** – Ideal to ensure that true equilibrium has been achieved. However, shifting results have been observed for prolonged contact times.

As mentioned above, when looking at the particle level, both film and pore diffusion play a part in the rate of mass transfer (i.e., serial mass transfer limitations). As one increases the rate of agitation during a batch contact test the numerical value for the surface film diffusion coefficient increases. The net result is a shift towards being pore diffusion limited. For the new batch of CST (R9120-B) a comparison of the batch kinetics data versus VERSE simulations are presented in Figure B-3. As shown in Figure B-3 four VERSE simulations were performed where the surface film diffusion coefficient was sequentially increased by one order of magnitude each time. The unique contribution associated with film and pore diffusion is shown. Setting the film diffusion coefficient to 1.0 nearly completely removes the impact of film diffusion such that cesium loading is only pore diffusion limited. In contrast, when the film diffusion coefficient is set to 0.01, film diffusion greatly impacts cesium loading kinetics.

The batch contact kinetics data (i.e., shown as red circles) are in duplicate where a larger spread in the data shows up for shorter timed tests. This probably is due to increased sensitivity at the higher transfer rates occurring at shorter times. Greater agitation is required at the shorter times

and adequate agitation may become unachievable using batch contact test methods at very short times. For contact times beyond approximately 100 hours, film diffusion no longer plays a role.

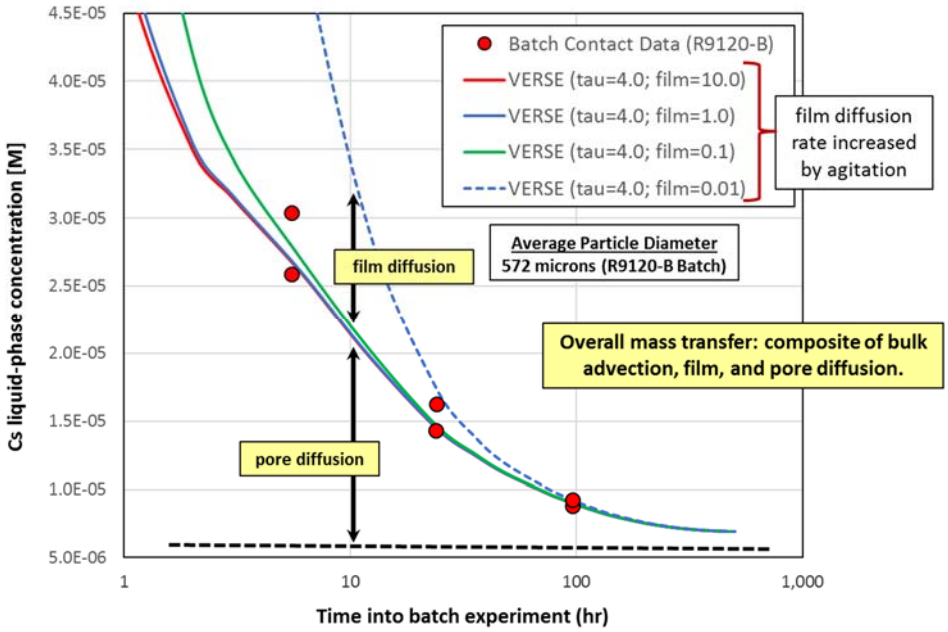

Figure B-3. CST (R9120-B) particle kinetic data versus VERSE modeling highlighting film versus pore diffusion contributions.

The primary reason for performing batch kinetics testing is to help in extracting a pore diffusion coefficient. The effective Cs^+ pore diffusion coefficient is dependent on:

- the CST media pore structure (i.e., CST batch specific) and
- the mobility of ions to free stream migration (i.e., liquid-phase properties)

The pore structure aspects are wrapped up into what is referred to as a "tortuosity factor" defined as:

$$\tau = \frac{D_{Cs}^{pore}}{D_{Cs}^{\infty}} \qquad \text{(B-1)}$$

where τ - Cs^+ tortuosity factor (Hamm, et al., 2002),

D_{Cs}^{∞} - liquid-phase free-stream Cs^+ diffusion coefficient, (cm^2/min)

D_{Cs}^{pore} - liquid-phase pore Cs^+ diffusion coefficient, (cm^2/min)

Based on prior studies with recent (larger bead size) CST material (see Hamm et al., 2018) a τ value around 4.0 was shown to be adequate for column predictions of simulant and radioactive waste solutions studied at PNNL. This value was employed in the VERSE predictions shown in Figure B-3.

It is assumed that the tortuosity factor is an intrinsic property of a given CST batch. Thus, its value remains constant throughout its structure. It is anticipated that its value may change from batch to batch but the variation is expected not to differ significantly from batch-to-batch. The variation in tortuosity factor is expected not to change much based on a consistent type of average particle

diameter. Thus, for the same batch of CST and employing the same means of averaging particle sizes, we would not expect to see much variation in tortuosity factor value.

A comparison of kinetic data for the IE-911 batch and the R9120-B batch is provided in Figure B-4. The volume mean average diameters are:

- IE-911 – $\langle D \rangle_{vol}$ = 408 µm (see Table 3-5)
- R9120-B – $\langle D \rangle_{vol}$ = 572 µm (see Table 3-2)

As expected the overall response is faster for the smaller IE-911 material. Two different tortuosity factor values were considered (i.e., 4.0 and 5.0). As Figure B-4 shows VERSE predictions are not capturing the early time data even when attempts to pre-wet the material were implemented. It is speculated that at these early times agitation rates were not sufficient to maintain adequate film diffusion coefficients. A tortuosity factor of 4.0 fits the IE-911 data well, while a value slightly higher, say around 4.5 might be a better fit to the R9120-B.

We also consistently see VERSE overpredicting the mass transfer (indicating greater cesium uptake) versus the experimental kinetics data (i.e., times < 5 hours). As stated above agitation rates may not be sufficient at these earlier times. Also VERSE only represents the group of particles being tested by a single average particle size. This assumption may yield a systematic bias within the predictions.

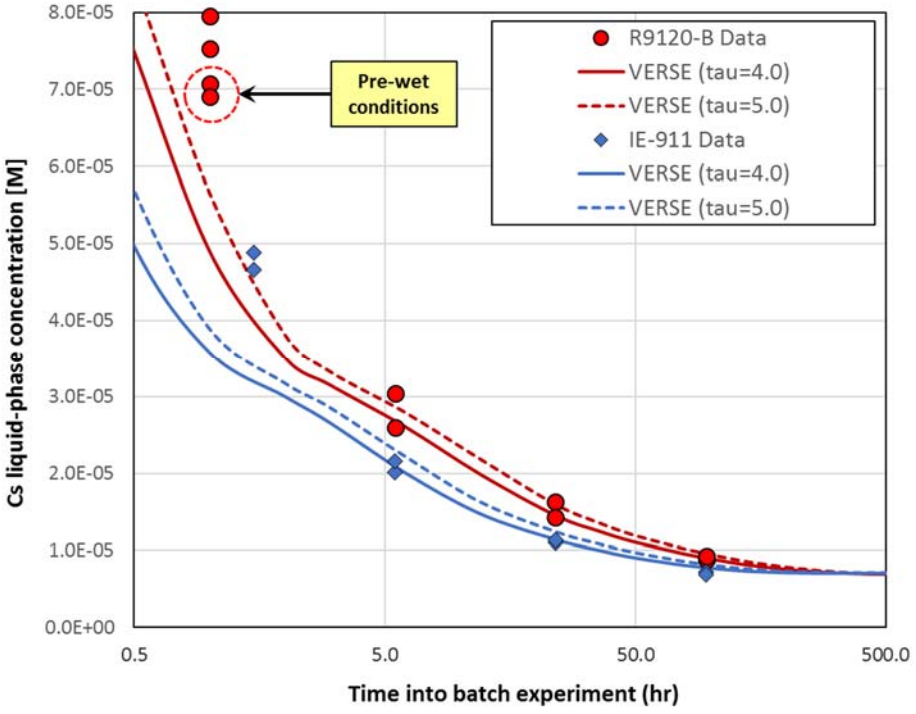

Figure B-4. CST (IE-911 and R9120-B) particle kinetic data versus VERSE modeling highlighting impact on particle size and batch differences.

To better see the tortuosity factor effect Figure B-4 is focused on contact times ranging from 5 to 500 hours and results for a value of 3.0 are included in Figure B-5. The tortuosity factor (geometric effect) is most likely batch dependent but not temperature or simulant dependent.

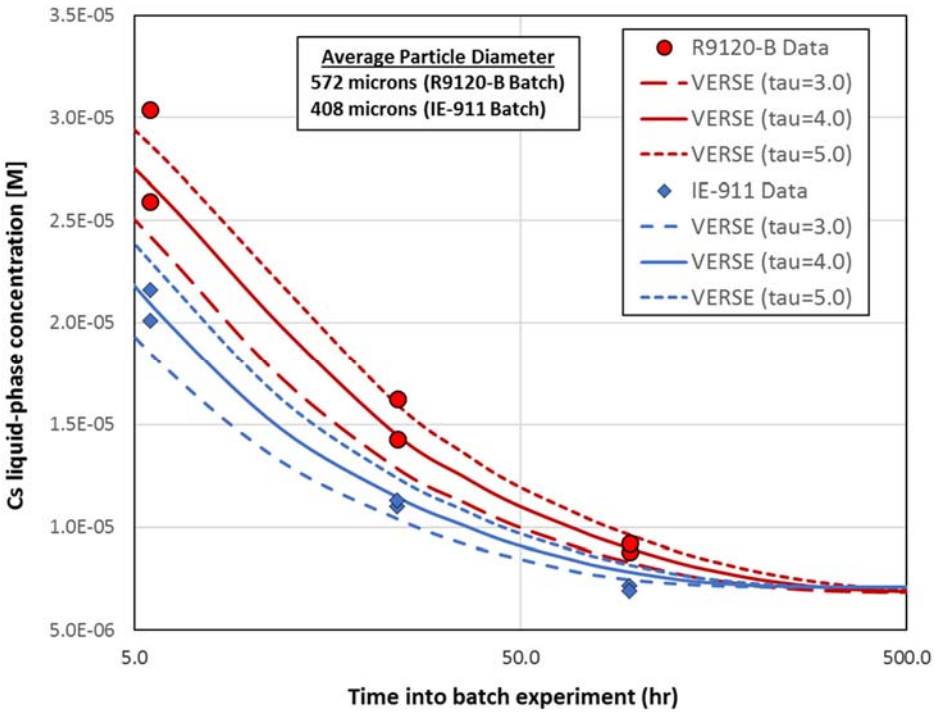

Figure B-5. CST (IE-911 and R9120-B) particle kinetic data versus VERSE modeling highlighting tortuosity factor impact.

Again, as Figure B-5 indicates a tortuosity factor of about 4.0 provides adequate coverage for both the IE-911batch (older material) and R9120-B batch (newer material). To better appreciate the rapid mass transfer rates that occur at early contact times, the above figure is replotted expanding out the vertical axis in Figure B-6. As Figure B-6 illustrates, significant Cs^+ concentration gradients are implied within CST particles (pore diffusion limited material). In Figure B-7 the entire response is shown starting from the initial Cs concentration in the liquid phase to the final near equilibrium Cs liquid-phase concentration. As Figure B-7 indicates a very rapid response is observed at the very short time periods.

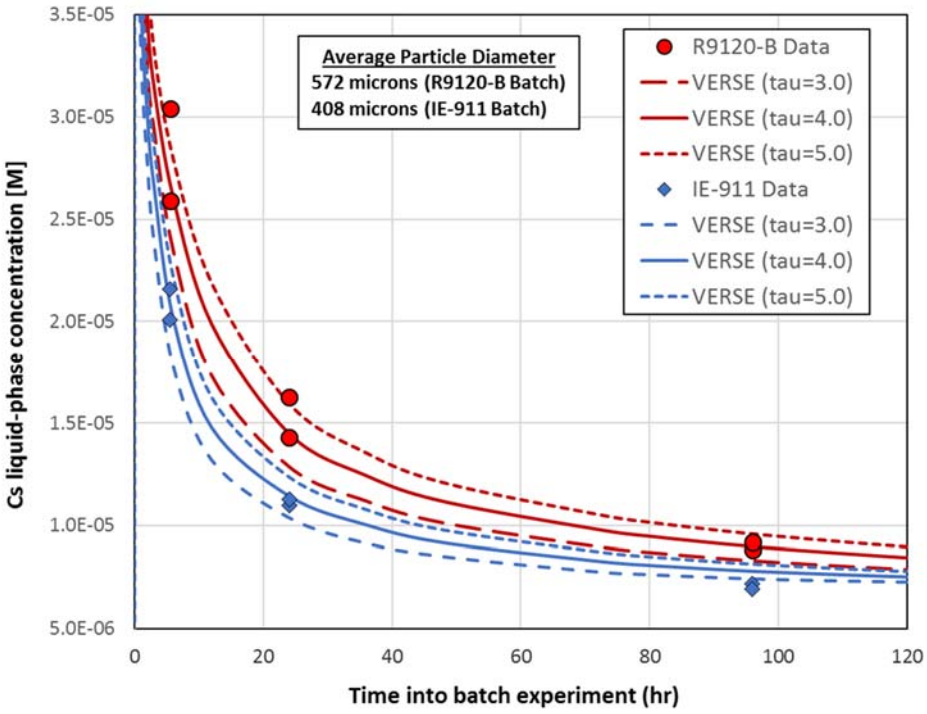

Figure B-6. CST (IE-911 and R9120-B) particle kinetic data versus VERSE modeling highlighting tortuosity factor impact at intermediate contact times.

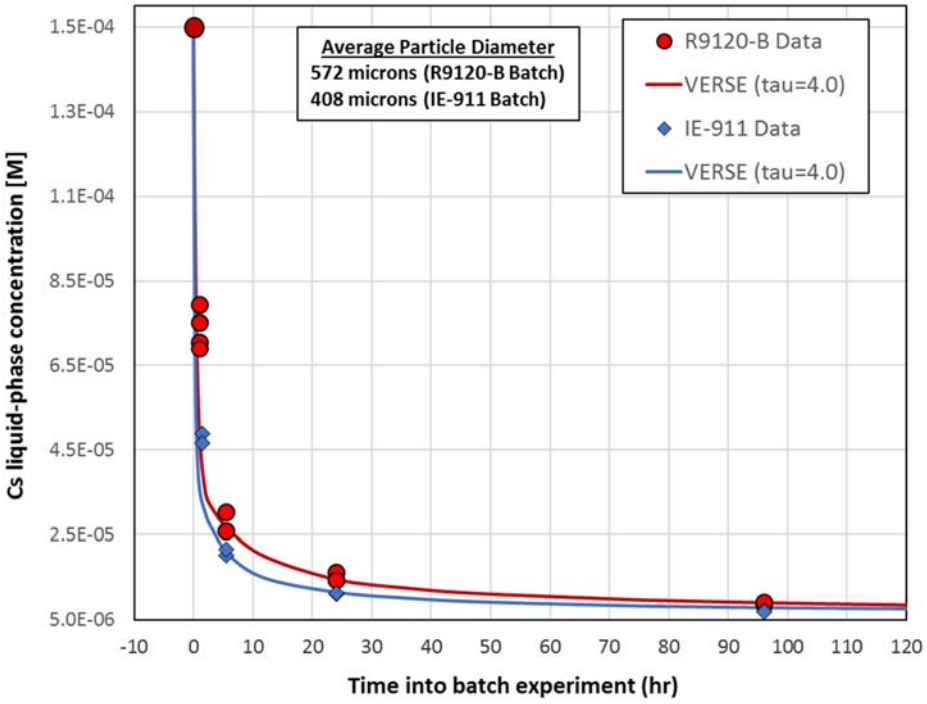

Figure B-7. CST (IE-911 and R9120-B) particle kinetic data versus VERSE modeling highlighting the rapid mass transfer rates at early times.

The actual numerical value of tortuosity factor is dependent upon what specific particle size metric one chooses to use. As provided in Table 3-2 and Table 3-5 various metrics can be chosen, and it

is important to establish a basis to select the best metric so that it can be used by all researchers in the future. To see this dependence VERSE simulations were made for IE-911 material for the three metrics (i.e., volume, surface, and number mean average) provided in Table 3-5. For each particle size metric VERSE calculations were performed with varying tortuosity factor values until a consistent response was achieved. The results on this series of VERSE calculations are provided in Figure B-8. As Figure B-8 indicates nearly identical responses can be achieved indicating that a specific tortuosity factor value is not unique until a particular particle size metric is chosen.

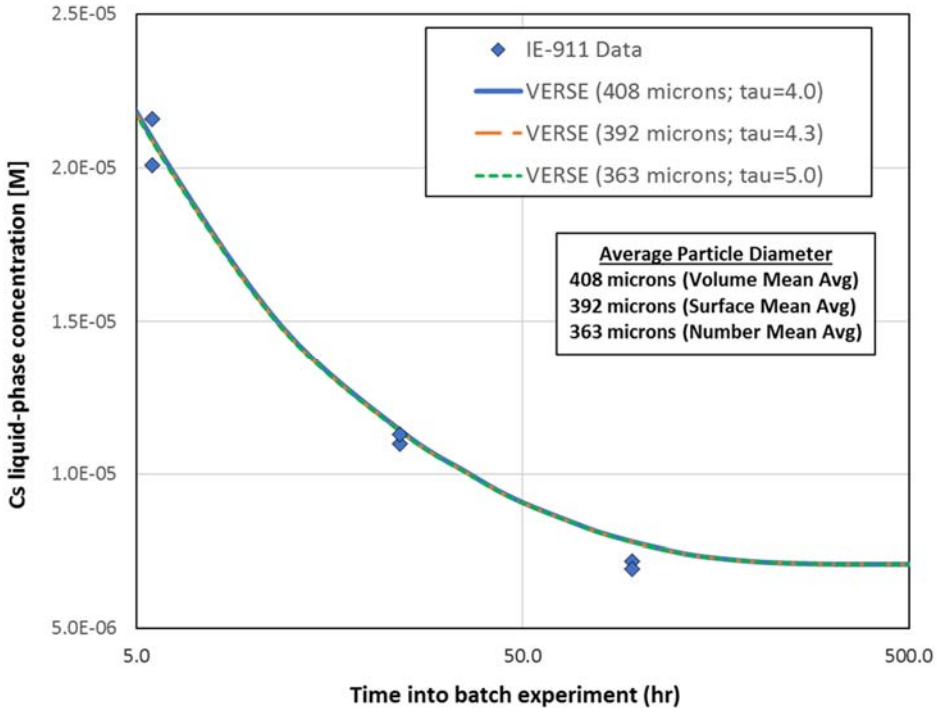

Figure B-8. Relationship between tortuosity factor value and what particle size metric chosen.

In fact, a correlation can be observed between the tortuosity factor and the particle size metric selected. For the three cases shown above a simple correlation exists as shown in Figure B-9.

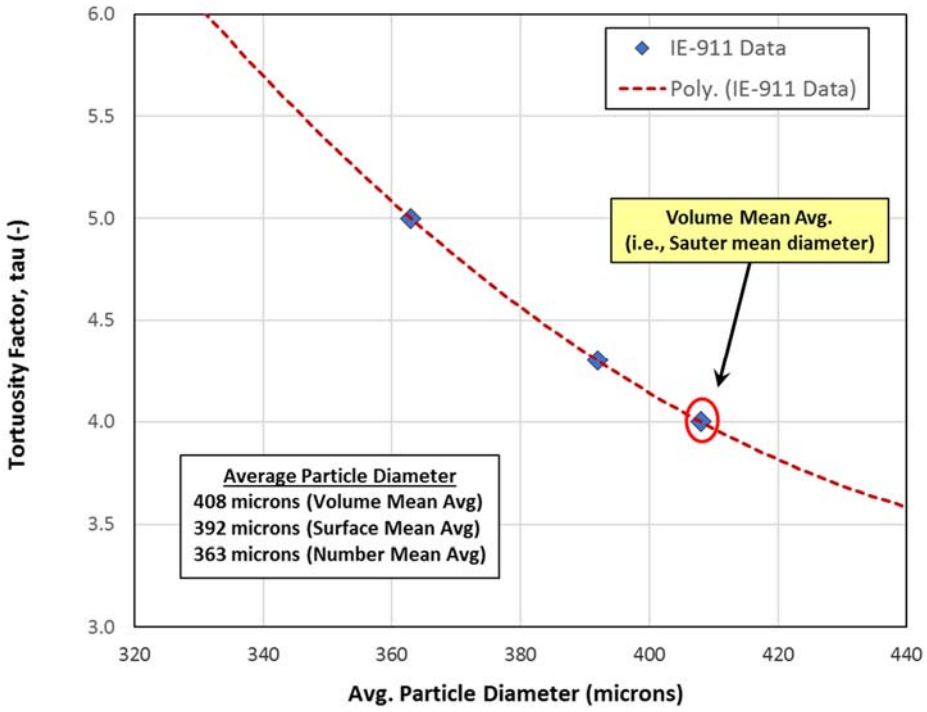

Figure B-9. Simple correlation between tortuosity factor and particle size metric for CST IE-911 material.

For the purposes of this report the volume mean average (i.e., Sauter mean) metric has been chosen. This is the metric generally preferred when computing mass transfer in packed beds.

Thus, a standard protocol for setting average particle diameter is required and based on the work performed in this effort we recommend sieve data and the Sauter mean.

Appendix C. CST Column Predictions/Performance

The VERSE code is being employed to perform CST column predictions to estimate Cs breakthrough performance for the TCCR project. VERSE has been SRNL's tool of choice for this since 2002 (for details see Hamm et al., 2002). VERSE has several configuration options as illustrated in Figure C-1.

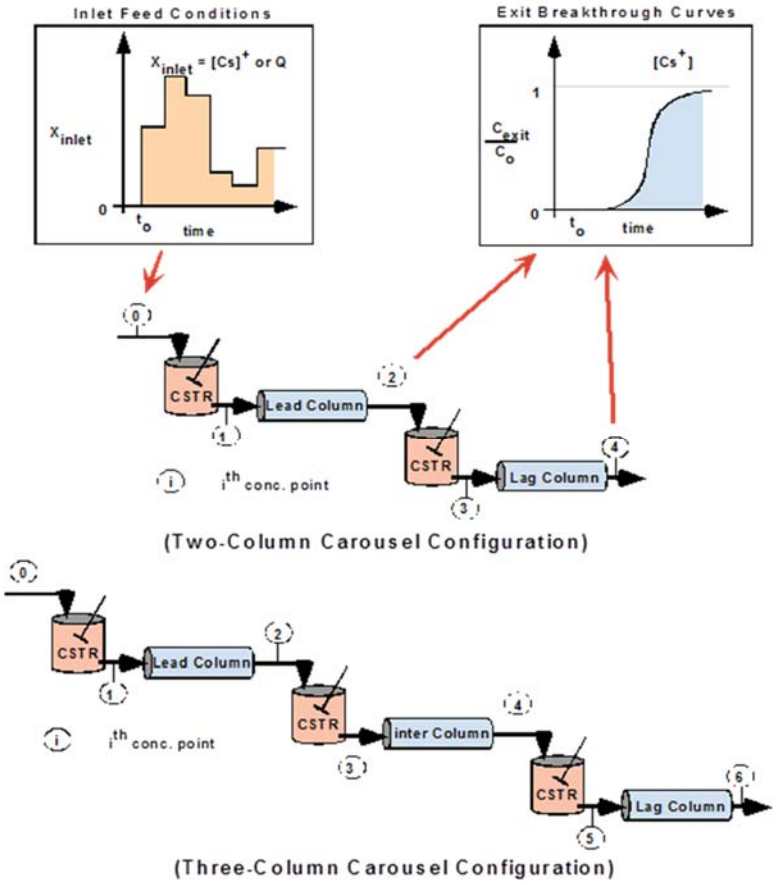

Figure C-1. Diagram showing a two-column and a three-column configuration in VERSE (2 column configuration used during initial TCCR operations but single column planned for laboratory testing).

For the work presented in this report only a single column configuration is considered. Upcoming SRNL laboratory-scale column testing in support of the TCCR project will focus on:

- Single column
- Fixed temperature
- Fixed flowrate
- Fixed feed composition
- Small effluent collection vessel (small sub-sample size/near instantaneous breakthrough)
- SRS Average Simulant
- Two CST batches with different particle diameter (IE-911 and R9120-B)

A series of single column VERSE simulations were made based on the proposed SRNL testing configuration. The following nominal parameter settings were employed:

- Cs feed = 2.0×10^{-5} [M]

- Temperature = 23°C
- Column ID = 1.75 cm
- Column length = 10.16 cm
- Column volume = 24.4 mL
- Bed L/D = 5.8
- CST avg particle diameter = 572 μm (R9120-B) and 408 μm (IE-911)
- Dry bulk bed density = 1.0175 g/ml[a] (R9120-B) and 1.0275 g/ml (IE-911)
- Bed porosity = 0.548
- Particle porosity = 0.24
- Tortuosity factor = 4.0
- Cs free-stream diffusivity = 5.586×10^{-4} cm^2/min
- Liquid density = 1.2275 g/ml
- Liquid absolute viscosity = 2.54701 cP
- Binder Dilution Factor = 0.76 (R9120-B) and 0.95 (IE-911)
- Isotherm parameter a value = 0.44851 mmol/ml (R9120-B) and 0.56615 mmol/ml (IE-911)
- Isotherm parameter beta factor = 2.346×10^{-4} [M]

A limited number of off-nominal case calculations were also made:

- Temperature = 23, 30, and 40 °C
- Tortuosity factor (tau) = 3.5, 4.0, and 5.0
- Flowrate = 1.0, 2.0, 3.0, 4.0, and 6.0 BV/hr

For most of these simulations two Cs breakthrough plots were created:

- Semi-log plot – this graph provides details showing the volume of feed processed (in terms of BVs) when an instantaneous exit breakthrough reaches a decontamination factor of 1000.
- Linear plot – this graph shows the overall shape of the Cs breakthrough curve indicating the point of 50% breakthrough and how challenged the column is under current conditions (i.e., when not significantly mass transfer limited nice symmetrical S-shaped curves should be observed).

The VERSE results for the nominal case are shown in Figure C-2 (semi-log plot) and Figure C-3 (linear plot). As expected, the Cs breakthrough curves had a significantly reduced performance for the newer CST material due to its significantly larger average particle size. As Figure C-2 indicates, a factor of >2 earlier breakthrough at a decontamination factor of 1000 is observed. This is a direct result of pore limited kinetics and larger particle size rather than some intrinsic change the material performance.

[a] Note the comments in the main document text regarding the discovery of an error in the R9120-B f-factor that was not corrected in the modeling results. The actual bulk dry bed density of R9120-B was 0.9892 g/mL versus the value of 1.0175 g/mL used for modeling.

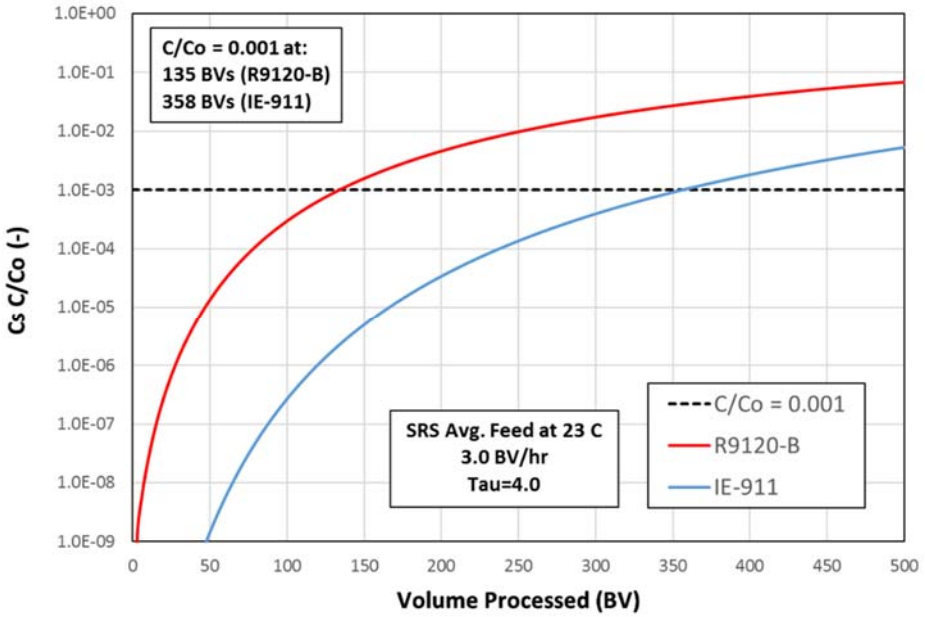

Figure C-2. VERSE predicted basecase Cs breakthrough curves based on single columns using IE-911 and R9120-B CST materials with SRS Average Simulant feed at 23°C (semi-log plot).

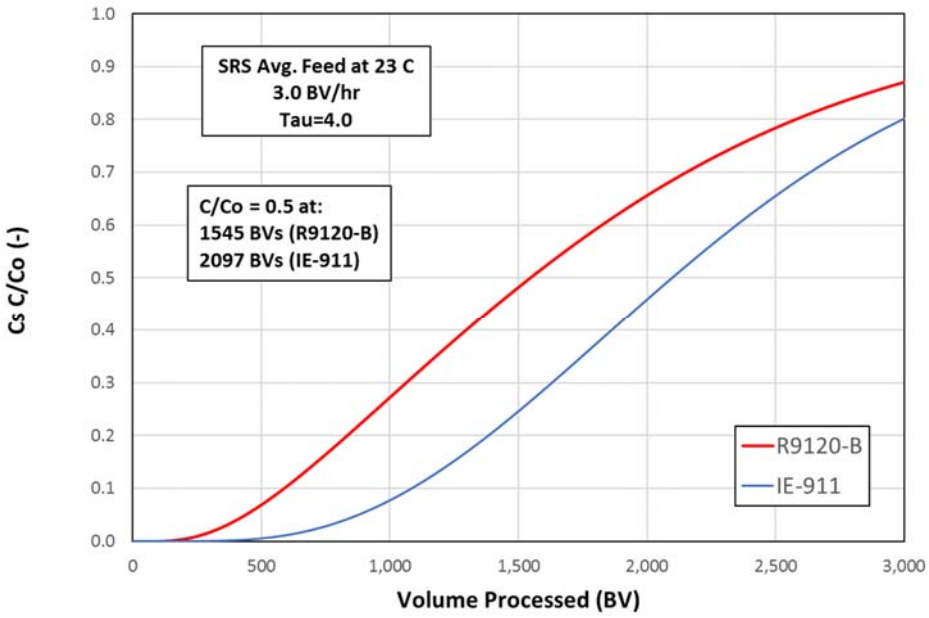

Figure C-3. VERSE predicted basecase Cs breakthrough curves based on single columns using IE-911 and R9120-B CST materials with SRS Average Simulant feed at 23°C (linear plot).

For the larger bead size R9120-B CST material, the VERSE results for a sensitivity study on the influence of temperature are shown in Figure C-4 (semi-log plot) and Figure C-5 (linear plot). As expected, the Cs breakthrough curves show overall performance reduction as the operating temperature is increased as shown in Figure C-5. However, when focusing in on performance with respect to the decontamination factor of 1000, little influence is seen as illustrated in Figure C-4. This is a result of the mass transfer limits on particle kinetics occurring where the leading edge of

the Cs breakthrough curve is dominated by cesium sorption kinetics rather than temperature influences upon the cesium loading isotherm. The opposing effects of isotherm loading shifts and cesium loading kinetic impacts on the breakthrough profiles at various temperatures result in a crossover of the profiles. The end result is minimal temperature impact on volume processed to reach the target DF.

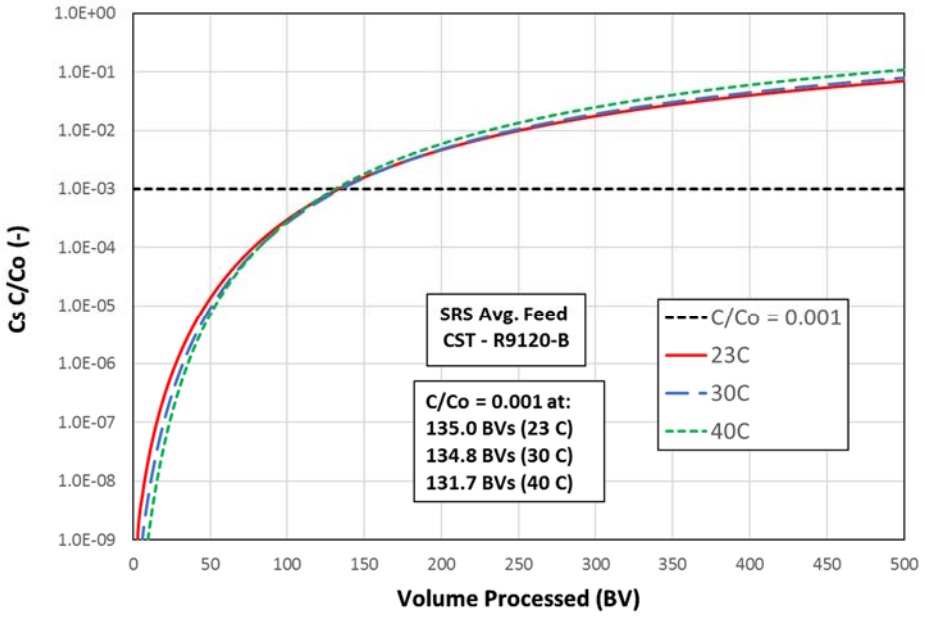

Figure C-4. VERSE predicted temperature impact on Cs breakthrough curves based on single columns using R9120-B CST material with SRS Average Simulant feed (semi-log plot).

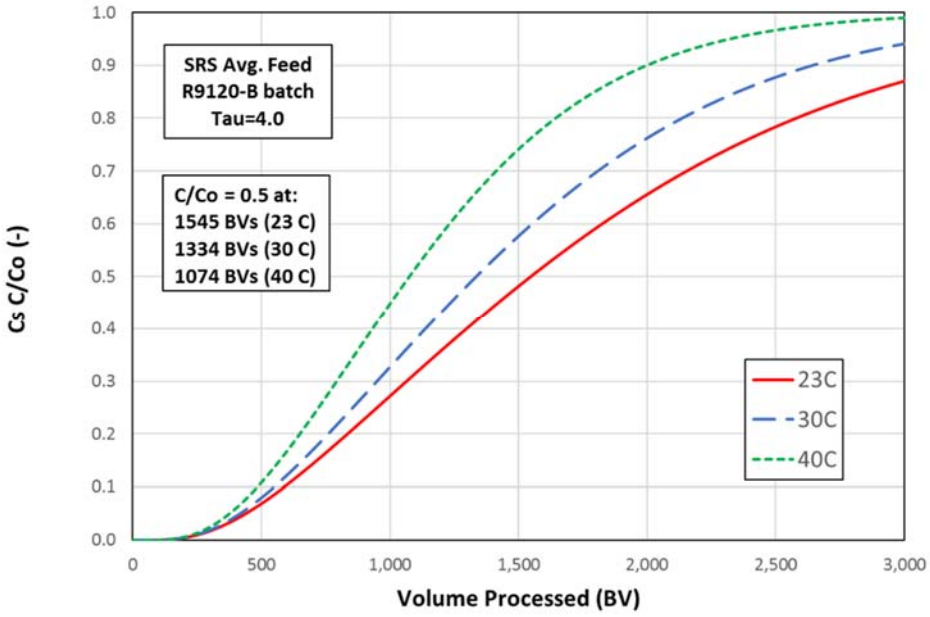

Figure C-5. VERSE predicted temperature impact on Cs breakthrough curves based on single columns using R9120-B CST material with SRS Average Simulant feed (linear plot).

For the newer R9120-B CST material the VERSE results for a sensitivity study on the influence of tortuosity factor are shown in Figure C-6 (semi-log plot). The tortuosity factor directly influences the particle kinetics which influences the performance with respect to the decontamination factor of 1000.

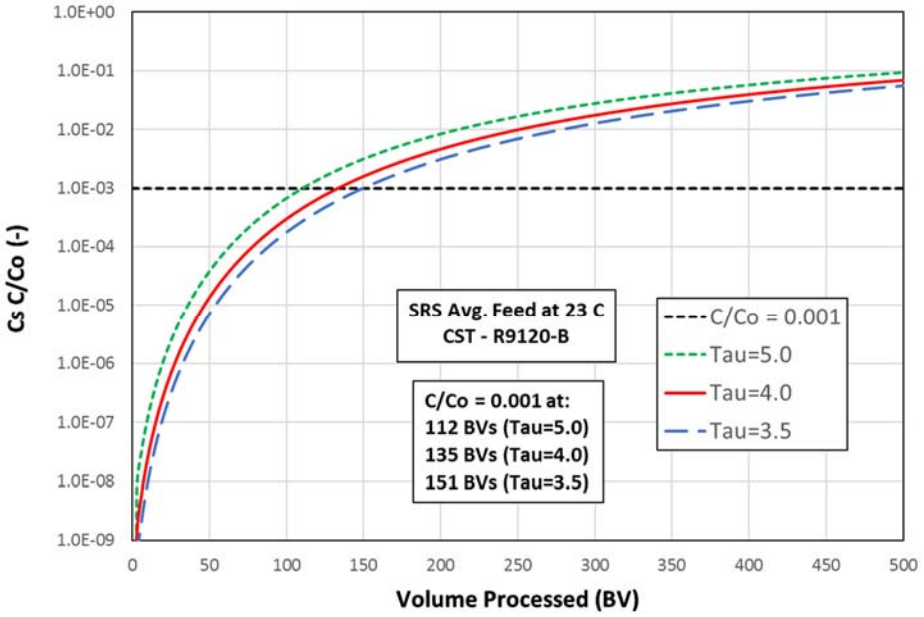

Figure C-6. VERSE predicted tortuosity factor impact on Cs breakthrough curves based on single columns using R9120-B CST material with SRS Average Simulant feed at 23°C (semi-log plot).

For the newer R9120-B CST material the VERSE results for a sensitivity study on the influence of flowrate is shown in Figure C-7 (semi-log plot) and Figure C-8 (linear plot). When focusing in on performance with respect to the decontamination factor of 1000, performance loss is seen as flowrate is increased as illustrated in Figure C-7. Again, increased flowrate leads to an increase in the degree of mass transfer limited behavior. When looking at the overall Cs breakthrough curves one sees (as expected) a shift in the inflection point to percent breakthrough values higher than 50% as shown in Figure C-8. As Figure C-8 indicates, as the flowrate is increased the S-shaped Cs breakthrough curves gradually begin to lose their S-shape.

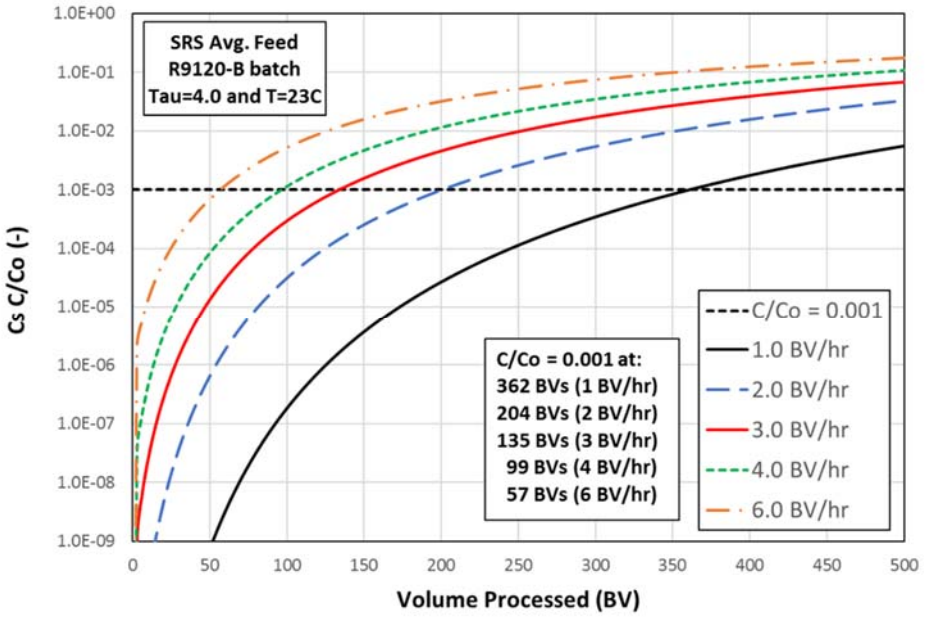

Figure C-7. VERSE predicted flowrate impact on Cs breakthrough curves based on single columns using R9120-B CST material with SRS Average Simulant feed at 23°C (semi-log plot).

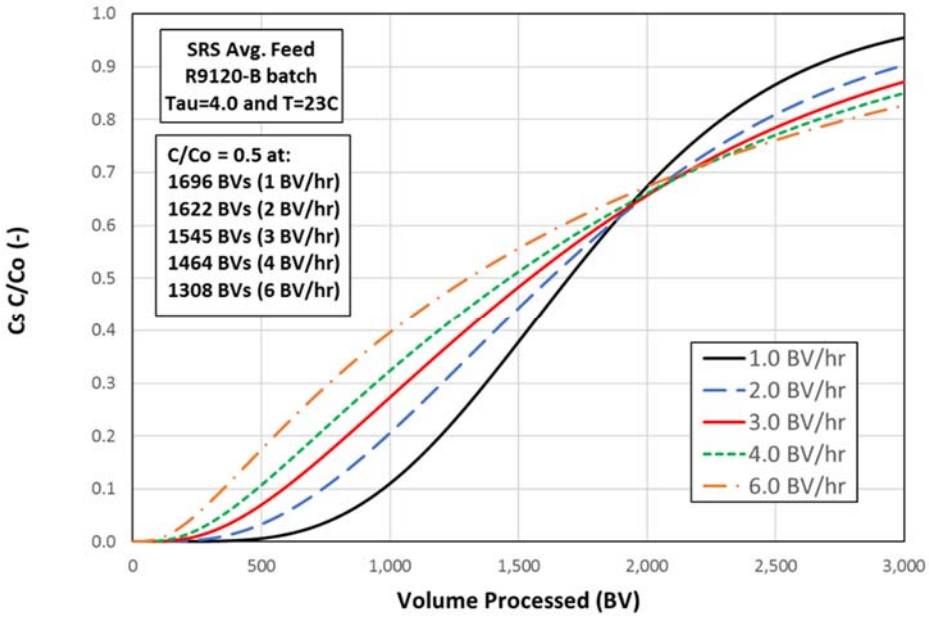

Figure C-8. VERSE predicted flowrate impact on Cs breakthrough curves based on single columns using R9120-B CST material with SRS Average Simulant feed at 23°C (linear plot).

Distribution:
timothy.brown@srnl.doe.gov
alex.cozzi@srnl.doe.gov
david.crowley@srnl.doe.gov
c.diprete@srnl.doe.gov
a.fellinger@srnl.doe.gov
samuel.fink@srnl.doe.gov
nancy.halverson@srnl.doe.gov
erich.hansen@srnl.doe.gov
connie.herman@srnl.doe.gov
Joseph.Manna@srnl.doe.gov
john.mayer@srnl.doe.gov
daniel.mccabe@srnl.doe.gov
Gregg.Morgan@srnl.doe.gov
frank.pennebaker@srnl.doe.gov
William.Ramsey@SRNL.DOE.gov
michael.stone@srnl.doe.gov
Boyd.Wiedenman@srnl.doe.gov
bill.wilmarth@srnl.doe.gov
chris.martino@srnl.doe.gov
william02king@srnl.doe.gov
richard.wyrwas@srnl.doe.gov
michael.stone@srnl.doe.gov
luther.hamm@srnl.doe.gov
charles.nash@srnl.doe.gov
amy.ramsey@srnl.doe.gov
kathryn.taylor-pashow@srnl.doe.gov
mark.keefer@srs.gov
richard.edwards@srs.gov
vijay.Jain@srs.gov
tony.polk@srs.gov
patricia.suggs@srs.gov
terri.fellinger@srs.gov
fmiera@charter.net
joseph_e_meacham@rl.gov
roger_d_lanning@rl.gov
kyle_d_hein@rl.gov
david_houghton@rl.gov
christopher_a_burke@rl.gov
rose_m_russell@rl.gov
pbogen@columbia-energy.com
bbrendel@columbia-energy.com
sfagnew@columbia-energy.com
schmoker@sterlingecg.com
kristopher_d_thomas@orp.doe.gov
nicholas_w_nick_kirch@rl.gov
michael.norato@em.doe.gov
linda.suttora@em.doe.gov
janet_a_diediker@orp.doe.gov
sahid.smith@orp.doe.gov
karthik_subramanian@rl.gov
cynthia_w_beaumier@rl.gov
matthew_r_landon@rl.gov
jason_r_vitali@rl.gov
kristin_a_colosi@rl.gov
stuart_t_arm@rl.gov
jacob_g_reynolds@rl.gov
Records Administration (EDWS)